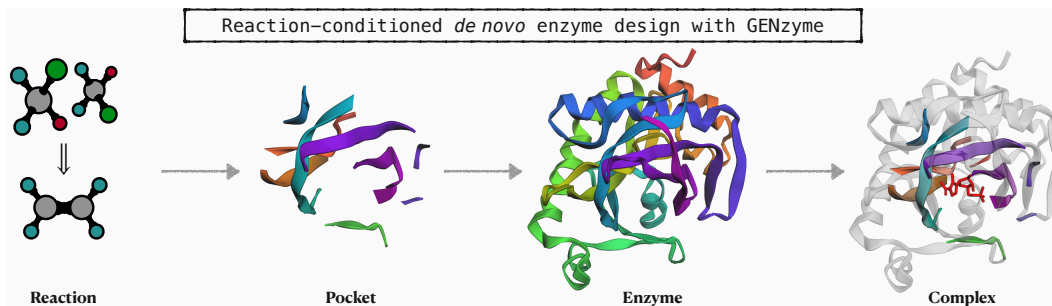


## REACTION-CONDITIONED DE NOVO ENZYME DESIGN WITH GENZYME

Chenqing Hua<sup>1,3,†\*</sup> Jiarui Lu<sup>3,4,†</sup> Yong Liu<sup>5</sup> Odin Zhang<sup>6</sup>Jian Tang<sup>3,4</sup> Rex Ying<sup>7</sup> Wengong Jin<sup>8,9</sup> Guy Wolf<sup>3,4</sup> Doina Precup<sup>1,3,10\*</sup> Shuangjia Zheng<sup>2\*</sup><sup>1</sup>McGill; <sup>2</sup>SJTU; <sup>3</sup>Mila-Quebec AI Institute; <sup>4</sup>UdeM; <sup>5</sup>HKUST;<sup>6</sup>Institute for Protein Design, UW; <sup>7</sup>Yale; <sup>8</sup>Northeastern; <sup>9</sup>Board & MIT; <sup>10</sup>DeepMind

## ABSTRACT

The introduction of models like RFDiffusionAA, AlphaFold3, AlphaProteo, and Chai1 has revolutionized protein structure modeling and interaction prediction, primarily from a binding perspective, focusing on creating ideal lock-and-key models. However, these methods can fall short for enzyme-substrate interactions, where perfect binding models are rare, and induced fit states are more common. To address this, we shift to a functional perspective for enzyme design, where the enzyme function is defined by the reaction it catalyzes. Here, we introduce GENZYME, a *de novo* enzyme design model that takes a catalytic reaction as input and generates the catalytic pocket, full enzyme structure, and enzyme-substrate binding complex. GENZYME is an end-to-end, three-staged model that integrates (1) a catalytic pocket generation and sequence co-design module, (2) a pocket inpainting and enzyme inverse folding module, and (3) a binding and screening module to optimize and predict enzyme-substrate complexes. The entire design process is driven by the catalytic reaction being targeted. This reaction-first approach allows for more accurate and biologically relevant enzyme design, potentially surpassing structure-based and binding-focused models in creating enzymes capable of catalyzing specific reactions. We provide GENZYME code at <https://github.com/WillHua127/GENzyme>.



## 1 INTRODUCTION

*“Congrats to David Baker, Demis Hassabis, and John Jumper for winning the 2024 Nobel Prize in Chemistry. Our research on AI-driven protein design would not have been possible without the groundbreaking contributions of their foundational work. We feel grateful for everything.” — by Authors*

Proteins are fundamental to life, playing an important role in numerous biological processes through their involvement in essential interactions (Whitford, 2013; Nam et al., 2024). Among these, enzymes stand out as a specialized class of proteins that function as catalysts, driving and regulating nearly all chemical reactions and metabolic pathways in living organisms, from simple bacteria to complex mammals (Kraut, 1988; Murakami et al., 1996; Copeland, 2023) (illustrated in Fig. 1(A)). The catalytic efficiency of enzymes is central to biological functions, facilitating the rapid production of complex organic molecules necessary for biosynthesis (Liu & Wang, 2007; Ferrer et al., 2008; Reetz

\*Corresponding author. † Co-authorship.

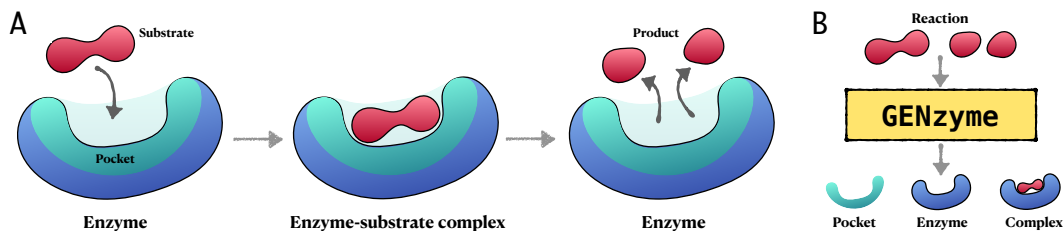


Figure 1: (A) Enzyme-substrate interaction mechanism. The substrate molecule binds to the enzyme catalytic pocket, where it undergoes catalysis and is converted into product molecules. (B) The overarching goal of GENZYME for *de novo* enzyme design. Starting from a catalytic reaction, it generates the catalytic pocket, complete enzyme structure, and the enzyme-substrate complex.

et al., 2024) and enabling the creation of novel biological pathways in synthetic biology (Keasling, 2010; Hodgman & Jewett, 2012; Girvan & Munro, 2016). Studying enzyme functions across diverse species provides insight into the evolutionary mechanisms that shape metabolic networks, allowing organisms to adapt to their environments (Jensen, 1976; Glasner et al., 2006; Campbell et al., 2016; Pinto et al., 2022). Enzymes are integral to cellular functions, from energy production to the regulation of genetic information (Babcock & Wikström, 1992; Heinrich & Schuster, 2012; Nielsen & Keasling, 2016). Understanding enzyme catalysis, mechanisms, and how enzymes interact with their substrates is not only fundamental to enhance our knowledge of core biological processes but also important for advancing biotechnology and developing new therapeutic approaches to disease management (Nam et al., 2024; Bell et al., 2024; Listov et al., 2024).

While traditional approaches in enzyme research have focused on predicting enzyme functions, annotating enzyme-reaction relationships (Gligorijević et al., 2021; Yu et al., 2023b), or retrieving enzyme-reaction pairs (Mikhael et al., 2024; Hua et al., 2024c; Yang et al., 2024b), these methods are limited in their ability to design new enzymes capable of catalyzing specific biological reactions (Kroll et al., 2023). Recent progress in designing enzymes for particular enzyme commission (EC) classes (Munsamy et al., 2022; Yang et al., 2024a) has shown success, with models generating enzyme sequences that closely resemble reference sequences and achieve desired EC classifications. Additionally, Hossack et al. (2023) introduced a method for designing novel enzymes by assembling active site and scaffold libraries, followed by refinement algorithms.

However, these advancements are not without limitations. Designing enzymes based solely on EC classifications can constrain model ability to generalize to novel, unseen reactions. In response, recent models have sought to move away from the EC system, instead aiming to directly comprehend the relationships between enzyme structures and their substrate molecules (Mikhael et al., 2024; Yang et al., 2024b; Hua et al., 2024c). Another significant challenge is that existing enzyme sequence design models are not yet equipped to comprehend the enzyme-substrate catalytic mechanism. Even when new enzyme sequences fold correctly into 3D structures, the catalytic pocket and the intricate binding interactions between enzymes and substrates are frequently underexplored or unclear.

In this work, we introduce GENZYME, a framework designed to address these challenges by generating enzymes capable of catalyzing previously unseen reactions (illustrated in Fig. 1(B)). Moreover, GENZYME aims to address the key question of how enzymes and substrates interact by generating enzyme-substrate binding structures. By leveraging generative models for enzyme scaffolds, active sites, and protein language models trained for enzyme motif scaffolding, GENZYME takes a catalytic reaction as input and generates the catalytic pocket, full enzyme structure, and enzyme-substrate complex. **GENZYME seeks to advance *de novo* enzyme design for specific catalytic reactions, enhance our understanding of enzyme active sites, and reveal how enzymes interact with substrates during catalysis—ultimately contributing to the understanding of metabolic pathways and potentially aiding therapeutic interventions and disease management.**

## 2 RELATED WORK—NOBEL-WINNING PROTEIN DESIGN MODELS

The field of AI-driven protein design was largely propelled by the success of AlphaFold (Senior et al., 2020), which achieved remarkable accuracy in protein structure prediction. AlphaFold2 (Jumper et al., 2021) further revolutionized the field, reaching experimental-level folding accuracy and solving the 50-year-old protein folding problem. This breakthrough provided millions of valid protein

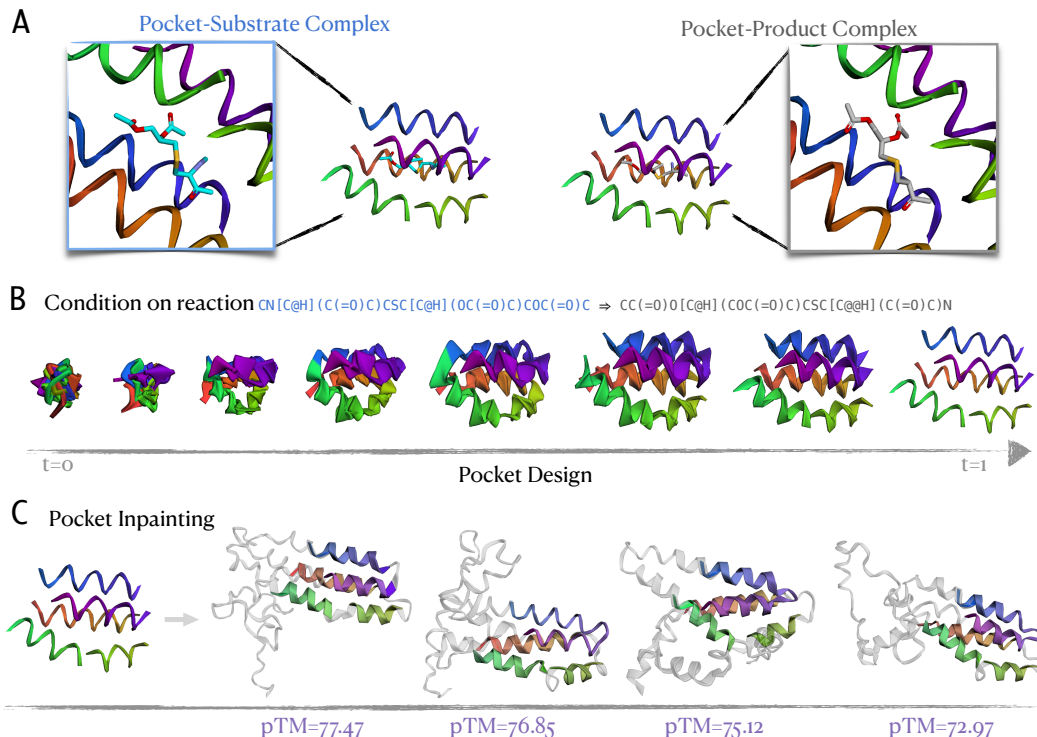


Figure 2: ***De novo* Enzyme Design with GENZYME.** (A) Pocket-substrate and pocket-product complexes generated by GENZYME, with the substrate molecule shown in cyan and the product molecule shown in gray. The positions of catalytic regions, substrate, and product conformations remain mostly unchanged after catalysis. (B) Reaction-conditioned iterative catalytic pocket generation with GENZYME. The catalytic pocket at  $t = 1$  (consists of 64 residues) is generated progressively from SE(3) noise initialized at  $t = 0$ . Additional visualizations are available in App. D.2. (C) Catalytic pocket inpainting with GENZYME, where the generated enzymes achieve high pTM scores, indicating structural quality and alignment with desired functions.

structure templates for nearly all catalogued proteins, a feat unattainable for decades. Similarly, RoseTTAFold (Baek et al., 2021) achieved high folding accuracy, comparable to AlphaFold2. These accomplishments were recognized with the Nobel Prize in Chemistry in 2024. OpenFold (Ahdritz et al., 2024), an open-source project inspired by AlphaFold2, aimed to make protein folding more accessible and transparent. ESMFold (Lin et al., 2022) applied ESM-series protein language models trained on millions of sequences, leveraging evolutionary information to predict protein structures at scale. ColabFold (Mirdita et al., 2022) streamlined the folding process by integrating AlphaFold2 and RoseTTAFold with MSAs, making protein structure prediction faster and easier via a web server.

These advancements in protein folding laid the foundation for structure-based protein design models. RFDiffusion (Watson et al., 2023) showcased the ability to generate novel protein structures—ranging from monomers to oligomers and binders—using a generative diffusion approach (Song et al., 2020). Other models, such as Genie (Lin & AlQuraishi, 2023), Chroma (Ingraham et al., 2023), FoldingDiff (Wu et al., 2024), FrameDiff (Yim et al., 2023b), FoldFlow (Bose et al., 2023), and EvoDiff (Alamdari et al., 2023), applied various diffusion and flow-matching (Lipman et al., 2022) strategies to design new proteins from random noise, demonstrating good novelty, diversity, and designability.

Beyond monomer designs, recent models have shifted toward designing proteins and their potential binders, including other proteins, molecules, antibodies, RNAs, and others. AlphaFold-Multimer (Evans et al., 2021) extended the folding models to predict protein complexes, learning how proteins interact with each other. RoseTTAFoldNA (Baek et al., 2024) was developed to predict 3D structures of protein-DNA and protein-RNA complexes, as well as RNA tertiary structures, capturing the interactions between proteins and nucleic acids. RFDiffusionAA (Krishna et al., 2024) enhanced RFDiffusion by incorporating all-atom representations, allowing it to generate detailed protein structures and ligand interactions. AlphaFold3 (Abramson et al., 2024) advanced AlphaFold2 by

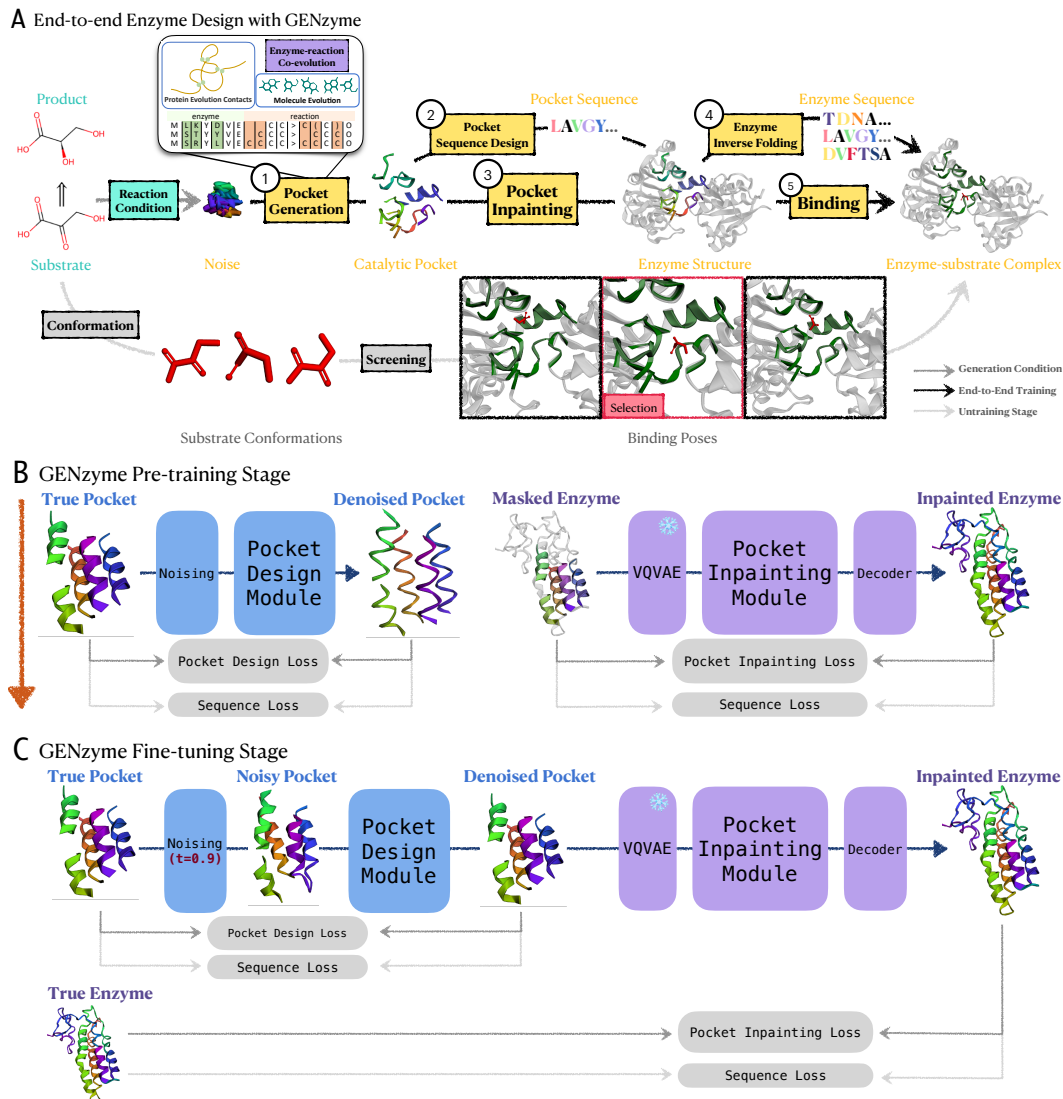
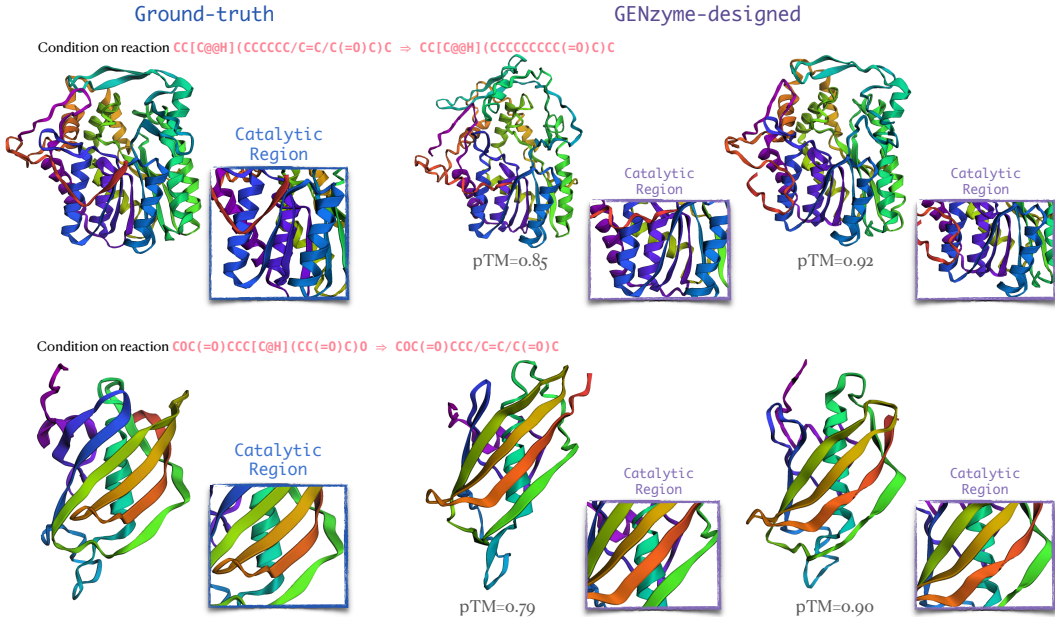


Figure 3: (A) **Reaction-conditioned enzyme design with GENZYME**. In example, the design process is conditioned on reaction  $\text{OCC(=O)C(=O)O} \Rightarrow \text{OC[C@H](C(=O)O)O}$ . GENZYME designs enzymes by first ① generating catalytic pockets, and ② co-designing pocket sequence. Next, it ③ inpaints the catalytic pocket to complete the full enzyme structure with ④ the generation of enzyme sequence. Finally, ⑤ the substrate conformation binds to the catalytic pocket of the full enzyme, and the ideal lock-and-key enzyme-substrate complex is predicted. (B) **GENZYME Pre-training Phase**, in which each module is trained individually on catalytic pockets and full enzyme structures. (C) **GENZYME Fine-tuning Phase**, where the model undergoes end-to-end training with slight perturbations applied to input pockets and enzymes.

predicting not only individual protein structures but also their interactions with DNA, RNA, and small molecules. Chai1 (Chai Discovery, 2024), inspired by AlphaFold3, offers an open-source web server for predicting protein interactions with other biological molecules, showing competitive results. AlphaProteo (Zambaldi et al., 2024) and BindCraft (Pacesa et al., 2024) focus on generating high-strength protein binders that can tightly bind to target molecules, such as viral or cancer proteins.

While structure-based protein design models are highly effective for creating stable and functional proteins, their primary focus is on static protein-ligand or protein-protein interactions. Enzymes, as catalysts that regulate nearly all chemical reactions and metabolic pathways in the human body, present a unique challenge for these models. Enzyme-substrate interactions are often driven by dynamic energy changes, and the induced-fit model is typically sufficient for catalysis. During

Figure 4: GENZYME *de novo* Enzyme Design Example.

a catalytic reaction, the enzyme transforms substrates into products through a chemical process, and afterward, it is free to bind another substrate molecule. The dynamic change and chemical transformation are completely different to static mechanism in protein-ligand interactions.

As a result, structure-based design models, which focus on static ligand-binding interactions, may fail to capture the dynamic transformations and complexities of enzyme-substrate interactions. In contrast, GENZYME proposes a function-based approach to enzyme design, where enzyme function is defined by the chemical reaction it catalyzes, potentially addressing the limitations of current structure-based models and allowing for the design of enzymes for specific catalytic functions.

Given any catalytic reaction  $m_r$ , GENZYME aims to generate/predict the enzyme  $\mathbf{E}$ , which is capable of potentially catalyzing  $m_r$ , and the corresponding enzyme-substrate complex  $\mathbf{C}$ , as:

$$\text{POCKET } \mathbf{E}^{\mathbf{P}}, \text{ ENZYME } \mathbf{E}, \text{ COMPLEX } \mathbf{C} \leftarrow \text{GENZYME}(\text{REACTION } m_r). \quad (1)$$

Fig. 3 illustrates the process by which GENZYME generates an enzyme and its corresponding docked enzyme-substrate complex. Starting with the input SMILES representations of the reaction, GENZYME generates the full enzyme structure and sequence from SE(3) noise, progressing through parts 1 to 4, where the catalytic pocket is first designed and then inpainted into a complete enzyme representation. Concurrently, the binding model computes multiple substrate conformations, optimizing both the geometry and binding poses based on the catalytic pocket of the full enzyme. An optimal enzyme-substrate model is predicted and output, as illustrated in part 5 of Fig. 3.

### 3 GENZYME RESULT

We evaluate GENZYME from both structural and functional perspectives, starting with an assessment of the quality of the generated catalytic pockets, followed by an evaluation of the inpainted full enzyme structures. GENZYME is compared against several baselines for enzyme design, including EnzymeFlow (pocket-level) (Hua et al., 2024b), ZymCTRL+ESMFold (enzyme-level) (Munsamy et al., 2022; Lin et al., 2022), and RFDiffusionAA (pocket- and enzyme-level) (Krishna et al., 2024). Additionally, we employ Chai1 (Chai Discovery, 2024) to assess the quality of enzyme-substrate complexes. For catalytic pockets and enzymes generated by RFDiffusionAA, we apply LigandMPNN (Dauparas et al., 2023) to inverse fold and predict sequences post-hoc.

For each model, we generate 8<sup>1</sup> catalytic pockets and full enzyme structures per reaction (or substrate for RFDiffusionAA, EC-class for ZymCTRL) to comprehensively evaluate their performance. For

<sup>1</sup>We limit sample generation to 8 due to wet-lab experimental constraints, as producing excessive samples is cost-prohibitive for laboratory trials. Typically, 3, 5, 8, or 10 samples are adequate for such trials.

Table 1: Evaluation data for enzyme design, featuring six enzyme-reaction pairs from different enzyme commission classes, representing a variety of functions, catalysis, and reaction types.

Enzyme	Substrate	Product
<b>03K145</b>	CC(C)CC(=O)OCC(=O)C	CC(=O)OCC(=O)OCC(=O)C
<b>03K147</b>	CC(C)CC(=O)OCC(=O)C	CC(C)CC(=O)OCC(=O)C
<b>03K170</b>	CC(C)CC(=O)OCC(=O)C	CC(C)CC(=O)OCC(=O)C
<b>03K180</b>	CC(C)CC(=O)OCC(=O)C	CC(C)CC(=O)OCC(=O)C
<b>03K181</b>	CC(C)CC(=O)OCC(=O)C	CC(C)CC(=O)OCC(=O)C
<b>03K182</b>	CC(C)CC(=O)OCC(=O)C	CC(C)CC(=O)OCC(=O)C
<b>03K183</b>	CC(C)CC(=O)OCC(=O)C	CC(C)CC(=O)OCC(=O)C
<b>03K184</b>	CC(C)CC(=O)OCC(=O)C	CC(C)CC(=O)OCC(=O)C
<b>03K185</b>	CC(C)CC(=O)OCC(=O)C	CC(C)CC(=O)OCC(=O)C
<b>03K186</b>	CC(C)CC(=O)OCC(=O)C	CC(C)CC(=O)OCC(=O)C
<b>03K187</b>	CC(C)CC(=O)OCC(=O)C	CC(C)CC(=O)OCC(=O)C
<b>03K188</b>	CC(C)CC(=O)OCC(=O)C	CC(C)CC(=O)OCC(=O)C
<b>03K189</b>	CC(C)CC(=O)OCC(=O)C	CC(C)CC(=O)OCC(=O)C
<b>03K190</b>	CC(C)CC(=O)OCC(=O)C	CC(C)CC(=O)OCC(=O)C
<b>03K191</b>	CC(C)CC(=O)OCC(=O)C	CC(C)CC(=O)OCC(=O)C
<b>03K192</b>	CC(C)CC(=O)OCC(=O)C	CC(C)CC(=O)OCC(=O)C
<b>03K193</b>	CC(C)CC(=O)OCC(=O)C	CC(C)CC(=O)OCC(=O)C
<b>03K194</b>	CC(C)CC(=O)OCC(=O)C	CC(C)CC(=O)OCC(=O)C
<b>03K195</b>	CC(C)CC(=O)OCC(=O)C	CC(C)CC(=O)OCC(=O)C
<b>03K196</b>	CC(C)CC(=O)OCC(=O)C	CC(C)CC(=O)OCC(=O)C
<b>03K197</b>	CC(C)CC(=O)OCC(=O)C	CC(C)CC(=O)OCC(=O)C
<b>03K198</b>	CC(C)CC(=O)OCC(=O)C	CC(C)CC(=O)OCC(=O)C
<b>03K199</b>	CC(C)CC(=O)OCC(=O)C	CC(C)CC(=O)OCC(=O)C
<b>03K200</b>	CC(C)CC(=O)OCC(=O)C	CC(C)CC(=O)OCC(=O)C
<b>03K201</b>	CC(C)CC(=O)OCC(=O)C	CC(C)CC(=O)OCC(=O)C
<b>03K202</b>	CC(C)CC(=O)OCC(=O)C	CC(C)CC(=O)OCC(=O)C
<b>03K203</b>	CC(C)CC(=O)OCC(=O)C	CC(C)CC(=O)OCC(=O)C
<b>03K204</b>	CC(C)CC(=O)OCC(=O)C	CC(C)CC(=O)OCC(=O)C
<b>03K205</b>	CC(C)CC(=O)OCC(=O)C	CC(C)CC(=O)OCC(=O)C
<b>03K206</b>	CC(C)CC(=O)OCC(=O)C	CC(C)CC(=O)OCC(=O)C
<b>03K207</b>	CC(C)CC(=O)OCC(=O)C	CC(C)CC(=O)OCC(=O)C
<b>03K208</b>	CC(C)CC(=O)OCC(=O)C	CC(C)CC(=O)OCC(=O)C
<b>03K209</b>	CC(C)CC(=O)OCC(=O)C	CC(C)CC(=O)OCC(=O)C
<b>03K210</b>	CC(C)CC(=O)OCC(=O)C	CC(C)CC(=O)OCC(=O)C
<b>03K211</b>	CC(C)CC(=O)OCC(=O)C	CC(C)CC(=O)OCC(=O)C
<b>03K212</b>	CC(C)CC(=O)OCC(=O)C	CC(C)CC(=O)OCC(=O)C
<b>03K213</b>	CC(C)CC(=O)OCC(=O)C	CC(C)CC(=O)OCC(=O)C
<b>03K214</b>	CC(C)CC(=O)OCC(=O)C	CC(C)CC(=O)OCC(=O)C
<b>03K215</b>	CC(C)CC(=O)OCC(=O)C	CC(C)CC(=O)OCC(=O)C
<b>03K216</b>	CC(C)CC(=O)OCC(=O)C	CC(C)CC(=O)OCC(=O)C
<b>03K217</b>	CC(C)CC(=O)OCC(=O)C	CC(C)CC(=O)OCC(=O)C
<b>03K218</b>	CC(C)CC(=O)OCC(=O)C	CC(C)CC(=O)OCC(=O)C
<b>03K219</b>	CC(C)CC(=O)OCC(=O)C	CC(C)CC(=O)OCC(=O)C
<b>03K220</b>	CC(C)CC(=O)OCC(=O)C	CC(C)CC(=O)OCC(=O)C
<b>03K221</b>	CC(C)CC(=O)OCC(=O)C	CC(C)CC(=O)OCC(=O)C
<b>03K222</b>	CC(C)CC(=O)OCC(=O)C	CC(C)CC(=O)OCC(=O)C
<b>03K223</b>	CC(C)CC(=O)OCC(=O)C	CC(C)CC(=O)OCC(=O)C
<b>03K224</b>	CC(C)CC(=O)OCC(=O)C	CC(C)CC(=O)OCC(=O)C
<b>03K225</b>	CC(C)CC(=O)OCC(=O)C	CC(C)CC(=O)OCC(=O)C
<b>03K226</b>	CC(C)CC(=O)OCC(=O)C	CC(C)CC(=O)OCC(=O)C
<b>03K227</b>	CC(C)CC(=O)OCC(=O)C	CC(C)CC(=O)OCC(=O)C
<b>03K228</b>	CC(C)CC(=O)OCC(=O)C	CC(C)CC(=O)OCC(=O)C
<b>03K229</b>	CC(C)CC(=O)OCC(=O)C	CC(C)CC(=O)OCC(=O)C
<b>03K230</b>	CC(C)CC(=O)OCC(=O)C	CC(C)CC(=O)OCC(=O)C
<b>03K231</b>	CC(C)CC(=O)OCC(=O)C	CC(C)CC(=O)OCC(=O)C
<b>03K232</b>	CC(C)CC(=O)OCC(=O)C	CC(C)CC(=O)OCC(=O)C
<b>03K233</b>	CC(C)CC(=O)OCC(=O)C	CC(C)CC(=O)OCC(=O)C
<b>03K234</b>	CC(C)CC(=O)OCC(=O)C	CC(C)CC(=O)OCC(=O)C
<b>03K235</b>	CC(C)CC(=O)OCC(=O)C	CC(C)CC(=O)OCC(=O)C
<b>03K236</b>	CC(C)CC(=O)OCC(=O)C	CC(C)CC(=O)OCC(=O)C
<b>03K237</b>	CC(C)CC(=O)OCC(=O)C	CC(C)CC(=O)OCC(=O)C
<b>03K238</b>	CC(C)CC(=O)OCC(=O)C	CC(C)CC(=O)OCC(=O)C
<b>03K239</b>	CC(C)CC(=O)OCC(=O)C	CC(C)CC(=O)OCC(=O)C
<b>03K240</b>	CC(C)CC(=O)OCC(=O)C	CC(C)CC(=O)OCC(=O)C
<b>03K241</b>	CC(C)CC(=O)OCC(=O)C	CC(C)CC(=O)OCC(=O)C
<b>03K242</b>	CC(C)CC(=O)OCC(=O)C	CC(C)CC(=O)OCC(=O)C
<b>03K243</b>	CC(C)CC(=O)OCC(=O)C	CC(C)CC(=O)OCC(=O)C
<b>03K244</b>	CC(C)CC(=O)OCC(=O)C	CC(C)CC(=O)OCC(=O)C
<b>03K245</b>	CC(C)CC(=O)OCC(=O)C	CC(C)CC(=O)OCC(=O)C
<b>03K246</b>	CC(C)CC(=O)OCC(=O)C	CC(C)CC(=O)OCC(=O)C
<b>03K247</b>	CC(C)CC(=O)OCC(=O)C	CC(C)CC(=O)OCC(=O)C
<b>03K248</b>	CC(C)CC(=O)OCC(=O)C	CC(C)CC(=O)OCC(=O)C
<b>03K249</b>	CC(C)CC(=O)OCC(=O)C	CC(C)CC(=O)OCC(=O)C
<b>03K250</b>	CC(C)CC(=O)OCC(=O)C	CC(C)CC(=O)OCC(=O)C

GENZYME, we randomly generate and select 8 enzymes with p<sub>TM</sub> > 0.60 or p<sub>LDDT</sub> > 0.60<sup>2</sup> and use their corresponding catalytic pockets for evaluation. Both structural validity and catalytic functionality are assessed for the generated pockets and enzymes. We provide the code of GENZYME and inference scripts at <https://github.com/WillHua127/GENzyme>.

**Evaluation Data.** For model validation, we select five enzyme-reaction pairs from each EC class (1-6) in the EnzymeFill dataset (Hua et al., 2024b), capturing diverse enzyme functions, catalytic mechanisms, and reaction types (Schomburg et al., 2002). Using MMseqs2 (Steinegger & Söding, 2017), we cluster at a 10% homology threshold and select the central member of each cluster as the initial dataset. After removing duplicates of repeated reactions and UniProt, we uniformly sample 5 enzyme-reaction pairs per EC class for evaluation, yielding a total of 30 unique catalytic pockets and 30 unique reactions. The full set of evaluation enzyme-reaction pairs is presented in Tab. 1.

### 3.1 ENZYME STRUCTURE EVALUATION

Following Hua et al. (2024b), we begin by evaluating the structural validity of the generated catalytic pockets and full enzymes. While enzyme function determines whether the designed pocket or enzyme can catalyze a specific reaction, structure provides important information regarding substrate binding. Proper substrate binding to the active region of the enzyme is essential for catalysis and chemical reaction, even if a perfect binding pose is not always needed.

To assess structural validity, we use the metrics: **Root Mean Square Deviation (RMSD)**: Measures the structural distance between ground-truth and generated catalytic pockets and enzymes, indicating the alignment accuracy of the generated structures with the actual structures. **TM-score**: Assesses topological similarity between generated and ground-truth structures, particularly focusing on local deviations (Zhang & Skolnick, 2005). **Embedding Distance (Emb-Dist)**: Calculates the embedding distance between generated and ground-truth pockets and enzymes. We co-encode both protein sequences and structures using ESM3 (Hayes et al., 2024), and employ tSNE to reduce hidden dimensionality to compute embedding distances.

We compare the structural validity of GENZYME- and baseline-generated catalytic pockets in Tab. 2, and the inpainted and generated enzymes in Tab. 3, focusing on structural consistency at both local (catalytic regions) and global (entire enzyme) levels.

In Tab. 2, which evaluates local consistency, GENZYME-generated catalytic pockets demonstrate closer alignment to ground-truth pockets, reflected in lower distance errors and higher structural alignment scores, as well as lower embedding distances. This suggests that GENZYME can design catalytic pockets that maintain or meet specific catalytic requirements for the target reaction. In Tab. 3, assessing global consistency, we observe that GENZYME-inpainted enzymes differ more from ground-truth structures than the catalytic regions alone, while the embedding distances do not diverge dramatically. This divergence indicates that, while GENZYME preserves critical catalytic properties locally, it also introduces structural modifications across the entire enzyme, potentially enhancing overall stability and functional diversity beyond wild-type enzymes.

These findings are further validated by the t-SNE visualizations in Fig. 5 and Fig. 6 in Sec. 3.2, where we analyze embeddings for generated catalytic pockets and full enzymes, supporting the observed balance between local catalytic alignment and broader structural innovation.

<sup>2</sup>We use a linear scheduler of p<sub>TM</sub> and p<sub>LDDT</sub> for filtering, starting with p<sub>TM</sub> > 0.80 or p<sub>LDDT</sub> > 0.80.

Table 2: Evaluation of structural validity of GENZYME- and baseline-generated catalytic pockets. We highlight the top performing results in **bold**.

Pocket Evaluation		RMSD ( $\downarrow$ )			TM-score( $\uparrow$ )			Emb-Dist( $\downarrow$ )		
		Top1	Top3	Mean	Top1	Top3	Mean	Top1	Top3	Mean
EC1	EnzymeFlow	3.76	3.90	4.19	0.29	0.28	0.26	19.82	20.29	21.48
	RFDiffusionAA	3.71	3.82	4.18	0.28	0.27	0.25	7.33	8.05	9.28
	GENZYME	<b>1.88</b>	<b>2.09</b>	<b>2.41</b>	<b>0.67</b>	<b>0.65</b>	<b>0.59</b>	<b>0.25</b>	<b>0.58</b>	<b>1.54</b>
EC2	EnzymeFlow	3.78	3.93	4.19	0.28	0.27	0.25	43.30	44.21	47.15
	RFDiffusionAA	3.47	<b>3.78</b>	4.17	0.27	0.27	0.25	26.91	27.84	30.44
	GENZYME	<b>3.65</b>	3.80	<b>4.09</b>	<b>0.33</b>	<b>0.31</b>	<b>0.28</b>	<b>1.03</b>	<b>1.85</b>	<b>4.40</b>
EC3	EnzymeFlow	3.46	3.69	4.12	0.31	0.29	0.27	9.84	10.02	11.14
	RFDiffusionAA	3.25	3.50	3.96	0.31	0.30	0.27	10.83	10.96	12.22
	GENZYME	<b>3.18</b>	<b>3.32</b>	<b>3.84</b>	<b>0.39</b>	<b>0.36</b>	<b>0.32</b>	<b>0.42</b>	<b>1.08</b>	<b>2.19</b>
EC4	EnzymeFlow	3.31	3.48	3.91	0.32	0.30	0.27	18.02	18.56	19.96
	RFDiffusionAA	3.00	3.29	3.79	0.30	0.29	0.27	14.62	15.62	17.39
	GENZYME	<b>2.58</b>	<b>2.73</b>	<b>2.96</b>	<b>0.56</b>	<b>0.54</b>	<b>0.51</b>	<b>0.50</b>	<b>1.07</b>	<b>2.43</b>
EC5	EnzymeFlow	3.48	3.66	4.06	0.29	0.28	0.26	13.71	14.01	14.81
	RFDiffusionAA	3.39	3.61	3.98	0.31	0.29	0.26	7.83	8.23	8.93
	GENZYME	<b>2.87</b>	<b>3.18</b>	<b>3.62</b>	<b>0.44</b>	<b>0.43</b>	<b>0.39</b>	<b>0.74</b>	<b>1.07</b>	<b>1.78</b>
EC6	EnzymeFlow	3.60	3.79	4.13	0.31	0.30	0.28	16.00	16.56	18.19
	RFDiffusionAA	3.43	3.69	4.12	0.30	0.29	0.26	19.08	19.73	21.21
	GENZYME	<b>3.14</b>	<b>3.32</b>	<b>3.73</b>	<b>0.43</b>	<b>0.40</b>	<b>0.36</b>	<b>1.23</b>	<b>1.45</b>	<b>2.56</b>

Table 3: Evaluation of structural validity of GENZYME-inpainted and baseline-generated enzymes. We highlight the top performing results in **bold**.

Enzyme Evaluation		RMSD ( $\downarrow$ )			TM-score( $\uparrow$ )			Emb-Dist( $\downarrow$ )		
		Top1	Top3	Mean	Top1	Top3	Mean	Top1	Top3	Mean
EC1	ZymCTRL+ESMFold	<b>3.48</b>	<b>4.08</b>	5.04	0.59	0.49	0.39	2.48	5.71	10.96
	RFDiffusionAA	4.46	4.76	5.36	0.48	0.44	0.38	22.38	23.79	26.89
	GENZYME	4.13	4.36	<b>4.83</b>	<b>0.62</b>	<b>0.58</b>	<b>0.53</b>	<b>2.41</b>	<b>2.92</b>	<b>5.49</b>
EC2	ZymCTRL+ESMFold	<b>4.74</b>	<b>5.05</b>	<b>5.51</b>	0.42	0.39	0.33	18.63	19.59	21.90
	RFDiffusionAA	4.88	5.08	5.58	<b>0.43</b>	<b>0.42</b>	<b>0.38</b>	5.42	6.31	8.91
	GENZYME	5.27	5.45	5.99	0.37	0.36	0.32	<b>5.15</b>	<b>6.25</b>	<b>8.43</b>
EC3	ZymCTRL+ESMFold	<b>4.87</b>	<b>5.02</b>	<b>5.47</b>	0.38	0.35	0.33	<b>1.61</b>	<b>4.65</b>	<b>10.82</b>
	RFDiffusionAA	5.13	5.28	5.71	0.38	0.36	0.33	4.95	6.74	10.59
	GENZYME	5.08	5.26	5.76	<b>0.38</b>	<b>0.38</b>	<b>0.33</b>	10.46	11.74	15.06
EC4	ZymCTRL+ESMFold	<b>3.92</b>	4.17	4.67	0.40	0.39	0.36	<b>2.95</b>	<b>5.98</b>	20.43
	RFDiffusionAA	4.49	4.68	5.25	0.45	0.42	0.37	65.60	69.49	78.31
	GENZYME	4.02	<b>4.15</b>	<b>4.59</b>	<b>0.57</b>	<b>0.55</b>	<b>0.52</b>	9.61	9.85	<b>10.49</b>
EC5	ZymCTRL+ESMFold	5.02	5.26	5.63	0.38	0.35	0.33	9.77	11.07	13.00
	RFDiffusionAA	<b>4.48</b>	<b>4.71</b>	<b>5.22</b>	<b>0.50</b>	<b>0.46</b>	<b>0.40</b>	<b>2.87</b>	<b>3.66</b>	<b>5.31</b>
	GENZYME	5.02	5.32	5.80	0.43	0.41	0.39	4.58	5.20	7.14
EC6	ZymCTRL+ESMFold	5.25	5.46	5.75	0.37	0.35	0.33	<b>5.97</b>	<b>7.88</b>	<b>13.25</b>
	RFDiffusionAA	<b>4.53</b>	<b>4.89</b>	<b>5.50</b>	<b>0.45</b>	<b>0.43</b>	<b>0.38</b>	19.38	20.76	25.87
	GENZYME	5.76	6.00	6.42	0.34	0.32	0.28	12.24	14.73	16.87

### 3.2 INSIGHTS FROM ENZYME SEQUENCE-STRUCTURE EMBEDDINGS

Additionally, we evaluate the generated catalytic pockets and full enzymes by analyzing their sequence-structure embeddings in comparison to ground-truth ones. We use ESM3 (Hayes et al., 2024) to co-encode both protein sequences and structures, though alternative methods like FoldSeek (van Kempen et al., 2022) are also viable for this purpose. Fig. 5 illustrates the tSNE visualization of catalytic pocket embeddings, and Fig. 6 presents the embeddings of full enzyme structures.

By analyzing Fig. 5, we observe that the GENZYME-generated catalytic pockets cluster closely with the ground-truth pockets, indicating high catalytic potential, as these active regions and catalytic sites are where reactions occur. This alignment suggests that GENZYME effectively maintains key

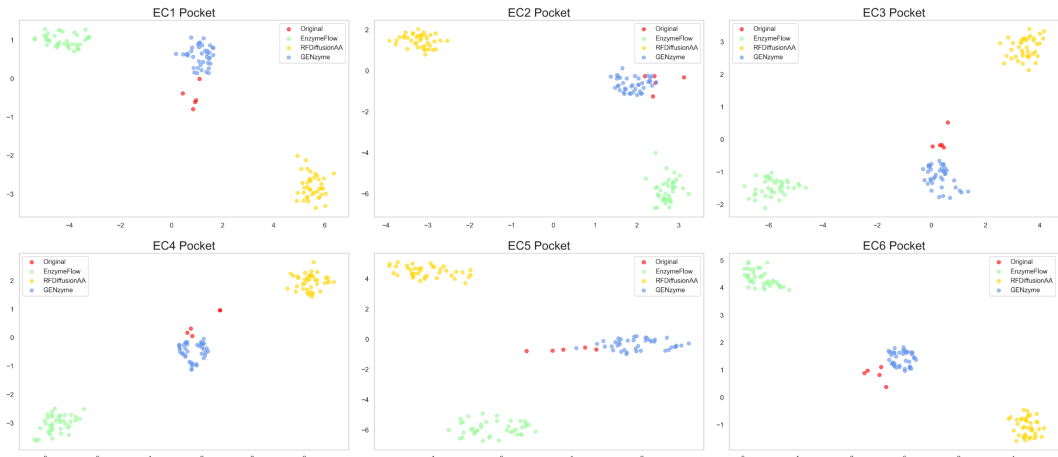


Figure 5: t-SNE visualization of **catalytic pocket embeddings** generated by ESM3. **Red** denotes ground-truth catalytic pockets, **yellow** denotes RFDiffusionAA-generated pockets, **blue** denotes GENZYME-generated pockets, and **green** denotes EnzymeFlow-generated pockets.

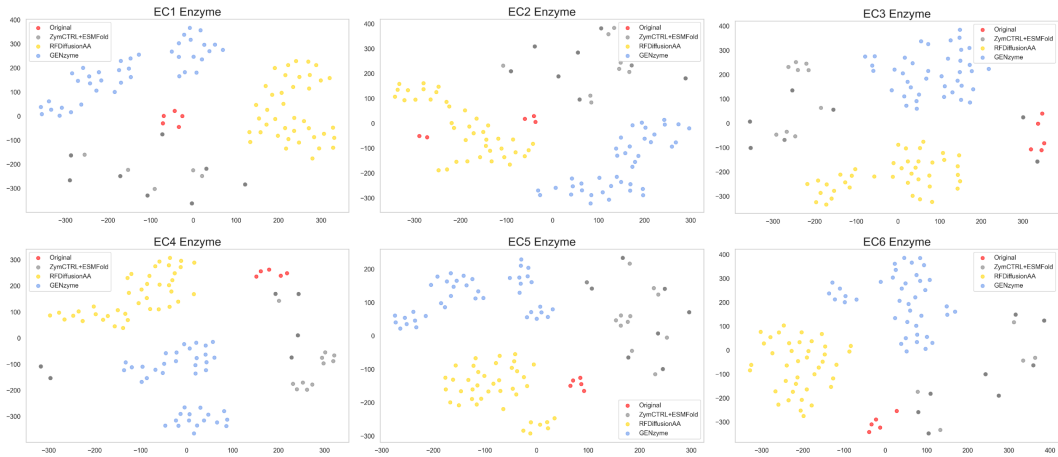


Figure 6: t-SNE visualization of **full enzyme embeddings** generated by ESM3. **Red** denotes ground-truth catalytic enzymes, **yellow** denotes RFDiffusionAA-generated enzymes, **blue** denotes GENZYME-generated enzymes, and **gray** denotes ZymCTRL+ESMFold-generated enzymes.

catalytic features. In contrast, Fig. 6 shows that the inpainted enzymes cluster separately from the ground-truth enzymes, which could imply enhanced overall enzyme stability and functionality in the *de novo* designs. Together, Fig. 5 and Fig. 6 suggest that GENZYME preserves essential catalytic properties while potentially improving overall enzyme stability and functional diversity.

### 3.3 ENZYME FUNCTION EVALUATION

A key question in enzyme design is how to *quantitatively* assess whether the generated catalytic pockets and enzymes can effectively catalyze a chemical reaction. To address this, we evaluate enzyme functions by analyzing the optimal pH, enzyme kinetics, and mutation effects of the generated pockets and full enzymes—three metrics that can provide insight into their catalytic potential.

First, we evaluate the **optimal pH** ( $pH_{opt}$ ), which refers to the specific pH level at which an enzyme achieves its highest catalytic activity. Although most enzymes perform optimally within a pH range of 6.0 to 8.0, some enzymes are specialized to function in highly acidic ( $pH_{opt} < 5.0$ ) or highly alkaline ( $pH_{opt} > 9.0$ ) conditions (Bisswanger, 2014). The pH affects enzyme activity by altering the enzyme shape and the charges at both the active site and substrate. For therapeutic applications, it is important that the enzyme functions well at physiological pH levels, or within the specific pH range of the tissue or fluid where it will act (Langer & Tirrell, 2004; Di Cera, 2009; Concolino et al., 2018). Therefore, we first evaluate the  $pH_{opt}$  of the designed enzymes to assess their functional suitability. To predict the optimal pH  $pH_{opt}$ , we use EpHod (Gado et al., 2023).



In addition to optimal pH, enzyme kinetics is a critical parameter for evaluating enzyme function. Specifically, we assess the **turnover number** ( $k_{\text{cat}}$ ), which describes the rate at which enzyme-catalyzed reactions occur. This metric provides insights into the enzyme’s catalytic mechanism, metabolic role, and responsiveness to potential inhibitors or activators (Wilkinson, 1961; Cornish-Bowden, 2013). The  $k_{\text{cat}}$  value, or turnover number, indicates the number of substrate molecules converted to product per second at each active site, thus reflecting the enzyme’s catalytic speed and efficiency. To predict and evaluate these kinetic parameters for the generated enzymes, we employ UniKP (Yu et al., 2023a), a tool that offers comprehensive insights into enzyme function and catalytic efficiency through kinetic profiling.

We also assess enzyme function by measuring the **rate of change of Gibbs free energy** ( $\Delta\Delta G$ ) **under mutation**, which quantifies the impact of mutation effects on enzyme stability relative to the wild-type enzymes (Romero & Arnold, 2009; Soskine & Tawfik, 2010). A negative  $\Delta\Delta G$  ( $\Delta\Delta G < 0$ ) indicates that the mutation increases stability, potentially enhancing enzyme fitness. A positive  $\Delta\Delta G$  ( $\Delta\Delta G > 0$ ) suggests decreased stability via mutation, which can reduce enzyme fitness. A zero  $\Delta\Delta G$  ( $\Delta\Delta G \approx 0$ ) implies that the mutation has little to no effect on stability. The enzyme fitness landscape, which maps the mutation effects on function and stability, can be better understood by analyzing  $\Delta\Delta G$ , as it helps predict whether a mutation will enhance or degrade the enzyme catalytic performance (Notin et al., 2024). To predict mutation effect  $\Delta\Delta G$ , we use Mutate-Everything (Ouyang-Zhang et al., 2024).

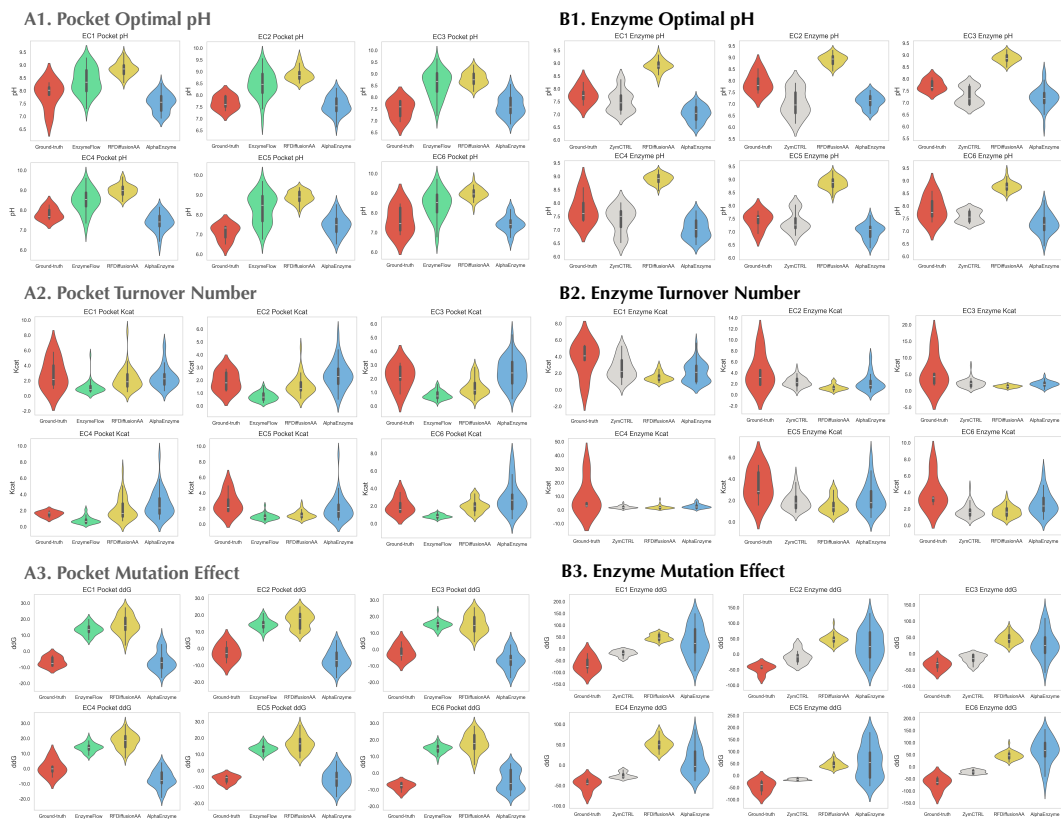


Figure 7: **Left: Pocket Function Evaluation.** (A1) Pocket optimal pH ( $pH_{\text{opt}}$ ). (A2) Pocket turnover number ( $k_{\text{cat}}$ ). (A3) Pocket mutation effects ( $\Delta\Delta G$ ). **Right: Enzyme Function Evaluation.** (B1) Enzyme optimal pH ( $pH_{\text{opt}}$ ). (B2) Enzyme turnover number ( $k_{\text{cat}}$ ). (B3) Enzyme mutation effects ( $\Delta\Delta G$ ). Red denotes ground-truth, green denotes EnzymeFlow-generated, yellow denotes RFDiffusionAA-generated, gray denotes ZymCTRL-generated, blue denotes GENZYME-generated.

In parallel to structural analysis, we assess the functional performance of GENZYME- and baseline-generated catalytic pockets in Fig. 7(left), as well as inpainted and generated enzymes in Fig. 7(right), examining functions at both local (catalytic regions) and global (entire enzyme) scales.

In evaluating optimal pH ( $pH_{opt}$ ) at both the catalytic pocket and full-enzyme levels, we observe that GENZYME produces pockets and enzymes that align more closely with the optimal pH values of ground-truth examples compared to those generated by baselines. This alignment is important, as catalytic reactions typically occur most efficiently at an enzyme’s optimal pH.

Regarding pocket turnover number ( $k_{cat}$ ), GENZYME generates catalytic pockets and enzymes with improved turnover rates relative to the ground truth and baseline models at the pocket level and outperforms baselines at the enzyme level. This improvement suggests higher catalytic efficiency from GENZYME-generated catalytic pockets.

For mutation effects ( $\Delta\Delta G$ ), at the pocket level, GENZYME-generated pockets demonstrate stability under mutation, indicating that mutations have minimal impact on structural stability and thus are unlikely to hinder catalytic performance. Additionally, GENZYME shows greater resilience to mutation effects at the enzyme level, suggesting an overall enhancement in stability. This reduced sensitivity to mutations implies that GENZYME designs can yield enzymes with more consistent functional stability across various conditions, further supporting stable catalytic activity.

## 4 GENZYME METHOD

We introduce GENZYME approach in App. B, C.

## 5 GENZYME DISCUSSION

GENZYME envisions a comprehensive approach to generating enzymes for specific catalytic reactions, aiming to contribute to therapeutic solutions, decompose harmful substances, and enhance our understanding of metabolic pathways. While it represents an important step forward, GENZYME is not yet a complete solution and does not reach the level of models like RFDiffusionAA (Krishna et al., 2024), AlphaFold (Jumper et al., 2021; Abramson et al., 2024), or AlphaProteo (Zambaldi et al., 2024). However, we hope that GENZYME can serve as a foundation for future advancements, inspiring further research and progress in *de novo* enzyme design, eventually leading to successful computational enzyme discovery and influencing therapeutics.

### 5.1 MODEL GENERALIZABILITY

We are currently testing GENZYME on the latest 2024 enzyme and reaction datasets collected from Rhea (Bansal et al., 2022), MetaCyc (Caspi et al., 2020), and Brenda (Schomburg et al., 2002). This will help us evaluate GENZYME’s performance and adaptability on newly collected, unseen data.

### 5.2 LIMITATIONS OF STRUCTURE-BASED MODELS FOR CATALYTIC REACTION MODELING

This section explores instances where structure-based protein and complex design models, including recent powerful methods like Chai-1 and AlphaFold3 (Chai Discovery, 2024; Abramson et al., 2024), occasionally fall short in accurately modeling catalytic reactions. A notable limitation in these complex generation models, particularly for our *de novo* enzyme design approach, is the requirement for an input protein sequence to generate the enzyme-substrate complex. However, for this analysis, we assume the enzyme sequence is known and focus solely on reaction modeling.

In our experiments using Chai-1 to model catalytic reactions, we observed a generally high success rate, where catalytic regions (active sites or catalytic pockets) remained stable and mostly unchanged throughout the catalytic process. Nonetheless, there are cases where Chai-1 does not maintain catalytic consistency, leading to significant alterations in catalytic regions.

Fig. 8 presents an example of such a failure, where Chai-1 does not preserve the original catalytic sites. The catalytic regions before the reaction (in blue) shift considerably after the reaction (in purple) for the resulting products. This illustrates that even advanced models like Chai-1 occasionally struggle with modeling catalytic reactions effectively. This finding highlights the need for a shift towards function-driven enzyme design, emphasizing catalytic activity as a primary objective—whether defined by specific reactions, as in our approach, or by enzyme classification systems like ZymCTRL’s EC-number-controlled generative strategy (Munsamy et al., 2022).

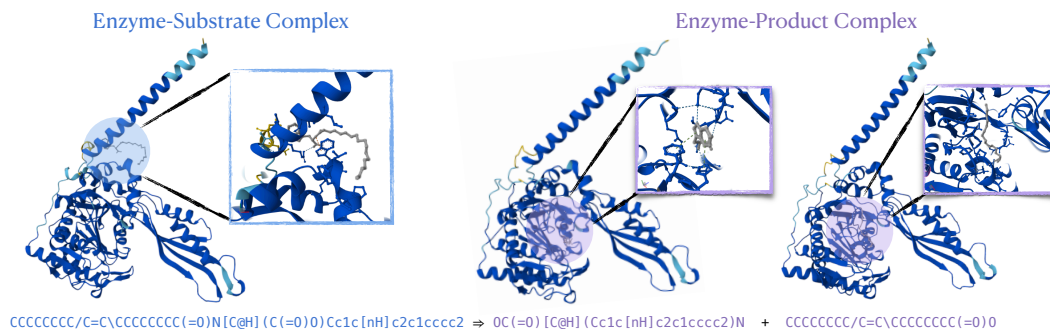


Figure 8: Catalytic reaction modeling for the enzyme of UniProt Q08BB2 using Chai-1.

### 5.3 WHAT DOES GENZYME AIM TO ADDRESS?

**Advancing *De Novo* Enzyme Design for Unseen Reactions.** GENZYME seeks to address the challenge of designing enzymes for novel, unseen catalytic reactions. This could deepen our understanding of metabolic pathways and offer therapeutic benefits, including disease intervention. By combining *de novo* catalytic pocket design, pocket inpainting, and protein evolutionary techniques, GENZYME attempts to generate new catalytic pockets both through computational design and biological mutation perspectives. This dual approach could make the algorithm more robust and generalizable to reactions that have not yet been experimentally observed.

**Shifting to Function-based Protein Design.** Unlike structure-based models such as RFDiffusionAA (Krishna et al., 2024), AlphaFold3 (Abramson et al., 2024), or Chai1 (Chai Discovery, 2024), which prioritize generating proteins based on structures, GENZYME aligns with a function-driven strategy. The input in GENZYME is defined by the enzyme function—the catalytic reaction it is meant to perform—rather than merely its structure. This approach emphasizes not only binding performance, *i.e.*, optimizing the enzyme-substrate binding affinities, but also ensures that the enzyme structure can facilitate the dynamic kinetic changes needed for catalysis. Although GENZYME encodes the protein function in a simplified way (via tokenized catalytic reactions), it introduces a novel direction for function-based protein design, where the function defines the structure.

**Addressing Data Scarcity in Enzyme Design.** A long-standing issue in enzyme design has been the lack of enzyme-reaction data with detailed structures or binding poses of enzyme-substrate complexes. Without this structural information, understanding how enzymes interact with substrates in the active site, and subsequently achieve catalysis, can be difficult. GENZYME attempts to address this challenge by generating synthetic enzyme-substrate complexes, which could provide insights into the mechanisms of catalysis and how enzymes facilitate specific reactions, helping bridge the gap in our understanding of enzyme-substrate interactions.

**Fine-tuned EnzymeESM for Representation Learning.** Beyond its focus on *de novo* enzyme design for therapeutic applications, GENZYME also contributes to enzyme representation learning. Current deep learning methods often employ models like ESM2 (Lin et al., 2022) or ProtT5 (Elnaggar et al., 2021) to embed enzymes for downstream tasks such as enzyme function prediction. Although these protein language models are pre-trained on millions of sequences, fine-tuning them for enzyme-specific tasks is necessary, similar to how large language models like LLaMa are fine-tuned for specific downstream applications (Howard & Ruder, 2018; Touvron et al., 2023). In this context, we fine-tune ESM3 (Hayes et al., 2024) on the EnzymeFill dataset, learning both enzyme sequences and structures. EnzymeESM is fine-tuned over 300,000 enzyme-reaction pairs, enabling tasks including enzyme catalytic pocket scaffolding, enzyme inverse folding, and enzyme embedding.

### 5.4 WHAT IS STILL MISSING IN GENZYME?

**Virtual Screening in Computational Enzyme Discovery.** A key gap in GENZYME, and in the broader field of computational enzyme discovery, is the lack of robust virtual screening models. Recent works have attempted to address this using contrastive learning methods to model enzyme-reaction relationships both from sequence and structural perspectives (Mikhael et al., 2024; Yang et al., 2024b; Hua et al., 2024c). However, current screening models remain insufficiently robust. Traditional approaches, such as using tools like Vina to compute binding affinities between enzymes

and substrate conformations (Trott & Olson, 2010), focus heavily on structural evaluations, which may not capture the full complexity of enzyme catalysis. An ideal virtual screening model, in our view, should take an enzyme-reaction pair as input and output a confidence score ranging from 0 to 1, indicating how likely the enzyme is to catalyze the reaction. This concept has been hinted at in earlier work Hua et al. (2024b). However, creating such a model presents significant challenges, particularly in generating meaningful negative enzyme-reaction pairs. For instance, CLIPZyme (Mikhael et al., 2024) treats all non-positive enzyme-reaction pairs as negative examples, while ReactZyme (Hua et al., 2024c) creates negative pairs by mutating amino acids in positive data. These methods are inspired by CLIP models in computer vision, where a mismatched image-text pair can clearly be labeled as negative (Radford et al., 2021). However, in enzyme-reaction prediction, an enzyme-reaction pair that does not exist in positive data could simply be an unobserved reaction, not necessarily a negative one. This limits the generalizability of current enzyme-reaction CLIP models, particularly for virtual screening of unseen enzyme-reaction pairs. We believe that improving virtual screening models in computational enzyme discovery is more important than generative models alone, as robust screening will enable the identification of truly functional enzyme-reaction pairs, enhancing the accuracy of enzyme design efforts.

**Integration of AI-assisted Protein Evolution.** Another missing aspect in GENZYME is the broader use of directed protein evolution, such as amino acid mutations, which are important for practical enzyme design (Arnold, 1998; Schmidt-Dannert & Arnold, 1999; Eijsink et al., 2005; King et al., 2024). Although GENZYME models enzyme-reaction co-evolution to account for dynamic changes in catalytic reactions, this is still insufficient from a practical, wet-lab perspective. In real-world experimental designs, researchers often start with enzyme mutations, rather than generating full enzyme structures from scratch. A more practical approach would be to focus on motif scaffolding—replacing active regions of existing enzymes with newly generated catalytic pockets, while preserving the rest of the enzyme backbone structure (Hossack et al., 2023). This method would align more closely with wet-lab needs, where scaffold-based modifications are often preferred due to higher success rates in enzyme design experiments. By designing enzymes from a scaffolding perspective, GENZYME could increase the likelihood of successful wet-lab implementation, ultimately bridging the gap between computational predictions and experimental outcomes.

## 5.5 BROADER IMPACT AND FUTURE WORK

The *de novo* enzyme design approach, while groundbreaking, naturally encounters limitations, particularly in verifying enzyme functionality. Although we are making strides toward addressing this through an enzyme evolution framework, our efforts remain in progress. Future work will focus on incorporating principles of enzyme engineering and site-specific mutations to enhance the functional reliability and catalytic efficiency of the *de novo* enzymes generated. These improvements aim to build a more robust and validated pathway for enzyme design, bridging the gap between computational predictions and real-world enzymatic applications.

A key challenge in enzyme design lies in accurately modeling substrate-product transitions, which are central to understanding catalytic mechanisms. Current approaches primarily focus on static binding models, yet dynamic interactions during catalysis remain underexplored. Future work will involve developing methods to model these substrate-product transitions more effectively, enabling designs that capture the full catalytic process. This could significantly improve the precision of *de novo* enzyme designs, bridging the gap between computational models and practical, functional enzymes capable of specific catalysis.

## ACKNOWLEDGEMENT

Chenqing thanks to the FACS-Acuity Project of Canada (No. 10242) and CIFAR AI Chairs, Shuangjia thanks to the National Natural Science Foundation of China (No. 62402314) and Aureka Bio. We extend our gratitude to Bozitao Zhong, Zuobai Zhang, Peter Mikhael, Hannes Stark, Sitao Luan for their valuable discussions and insights. We would like to acknowledge Mila and Nvidia for providing computational resources for the protein and enzyme experiments.

## CORRESPONDENCE

The paper corresponds to Chenqing Hua ([chenqing.hua@mail.mcgill.ca](mailto:chenqing.hua@mail.mcgill.ca)), Doina Precup ([dprecup@cs.mcgill.ca](mailto:dprecup@cs.mcgill.ca)), and Shuangjia Zheng ([shuangjia.zheng@sjtu.edu.cn](mailto:shuangjia.zheng@sjtu.edu.cn)).

## LICENSE

GENZYME is available under a Non-Commercial license.

## CONTRIBUTION STATEMENT

Chenqing contributes to the overall project, including proposing the workflow, coding, conducting experiments, and writing. Jiarui is responsible for fine-tuning ESM3 on the EnzymeFill. Yong contributes the data collection for EnzymeFill. Odin contributes to experiment validation. Jian provides supervision for Jiarui. Rex contributes to providing computational resources and writing. Wengong provides supervision. Guy and Doina provide support by securing computational resources, funding, and offering supervision. Shuangjia contributes to experimental validation, paper writing, and providing supervision.

## COMPETING INTERESTS

The authors claim no competing interests.

## REPRODUCIBILITY STATEMENT

We provide our code and example scripts with demonstrations at <https://github.com/WillHua127/GENzyme>.

## IMPACT STATEMENT

GENZYME aims to push the boundaries of *de novo* enzyme design, with potential applications in therapeutic applications and disease management. The next works include: (1) improving enzyme screening and filtering methods, (2) incorporating protein engineering and mutation strategies into the model, (3) augmenting data with enzyme kinetics, (4) integrating molecular dynamics, such as bond breaking, to better represent catalytic reaction conditions, (5) validating results through wet-lab experiments, and (6) training large-scale models.

## DATASET STATEMENT

We will soon release EnzymeFill data, in the spring or summer term of 2025.

## COLLABORATION STATEMENT

We welcome collaborations, inquiries, and discussions. Please feel free to reach out to us at [chenqing.hua@mail.mcgill.ca](mailto:chenqing.hua@mail.mcgill.ca) and [shuangjia.zheng@sjtu.edu.cn](mailto:shuangjia.zheng@sjtu.edu.cn). We are actively seeking experimentalists for wet-lab validation of *de novo* enzyme designs, as well as institutes or companies interested in providing additional data or computational resources to support large-scale training of GENZYME model.

## REFERENCES

- Josh Abramson, Jonas Adler, Jack Dunger, Richard Evans, Tim Green, Alexander Pritzel, Olaf Ronneberger, Lindsay Willmore, Andrew J Ballard, Joshua Bambrick, et al. Accurate structure prediction of biomolecular interactions with alphafold 3. *Nature*, pp. 1–3, 2024.
- Gustaf Ahdriz, Nazim Bouatta, Christina Floristean, Sachin Kadyan, Qinghui Xia, William Gerecke, Timothy J O’Donnell, Daniel Berenberg, Ian Fisk, Niccolò Zanichelli, et al. Openfold: Retraining alphafold2 yields new insights into its learning mechanisms and capacity for generalization. *Nature Methods*, pp. 1–11, 2024.
- Sarah Alamdari, Nitya Thakkar, Rianne van den Berg, Alex X Lu, Nicolo Fusi, Ava P Amini, and Kevin K Yang. Protein generation with evolutionary diffusion: sequence is all you need. *BioRxiv*, pp. 2023–09, 2023.
- Eric Alcaide, Zhifeng Gao, Guolin Ke, Yaqi Li, Linfeng Zhang, Hang Zheng, and Gengmo Zhou. Uni-mol docking v2: Towards realistic and accurate binding pose prediction. *arXiv preprint arXiv:2405.11769*, 2024.
- Mohammed AlQuraishi. End-to-end differentiable learning of protein structure. *Cell systems*, 8(4): 292–301, 2019.
- Stephen F Altschul, Warren Gish, Webb Miller, Eugene W Myers, and David J Lipman. Basic local alignment search tool. *Journal of molecular biology*, 215(3):403–410, 1990.
- Stephen F Altschul, Thomas L Madden, Alejandro A Schäffer, Jinghui Zhang, Zheng Zhang, Webb Miller, and David J Lipman. Gapped blast and psi-blast: a new generation of protein database search programs. *Nucleic acids research*, 25(17):3389–3402, 1997.
- Frances H Arnold. Design by directed evolution. *Accounts of chemical research*, 31(3):125–131, 1998.
- Jacob Austin, Daniel D Johnson, Jonathan Ho, Daniel Tarlow, and Rianne Van Den Berg. Structured denoising diffusion models in discrete state-spaces. *Advances in Neural Information Processing Systems*, 34:17981–17993, 2021.
- Gerald T Babcock and Märten Wikström. Oxygen activation and the conservation of energy in cell respiration. *Nature*, 356(6367):301–309, 1992.
- Minkyung Baek, Frank DiMaio, Ivan Anishchenko, Justas Dauparas, Sergey Ovchinnikov, Gyu Rie Lee, Jue Wang, Qian Cong, Lisa N Kinch, R Dustin Schaeffer, et al. Accurate prediction of protein structures and interactions using a three-track neural network. *Science*, 373(6557):871–876, 2021.
- Minkyung Baek, Ryan McHugh, Ivan Anishchenko, Hanlun Jiang, David Baker, and Frank DiMaio. Accurate prediction of protein–nucleic acid complexes using rosettafoldna. *Nature methods*, 21(1): 117–121, 2024.
- Amos Bairoch. The enzyme database in 2000. *Nucleic acids research*, 28(1):304–305, 2000.
- Parit Bansal, Anne Morgat, Kristian B Axelsen, Venkatesh Muthukrishnan, Elisabeth Coudert, Lucila Aimo, Nevila Hyka-Nouspikel, Elisabeth Gasteiger, Arnaud Kerhornou, Teresa Batista Neto, et al. Rhea, the reaction knowledgebase in 2022. *Nucleic acids research*, 50(D1):D693–D700, 2022.
- Elizabeth L Bell, Amy E Hutton, Ashleigh J Burke, Adam O’Connell, Amber Barry, Elaine O’Reilly, and Anthony P Green. Strategies for designing biocatalysts with new functions. *Chemical Society Reviews*, 2024.
- Hans Bisswanger. Enzyme assays. *Perspectives in Science*, 1(1-6):41–55, 2014.
- Jesse D Bloom and Frances H Arnold. In the light of directed evolution: pathways of adaptive protein evolution. *Proceedings of the National Academy of Sciences*, 106(supplement\_1):9995–10000, 2009.
- Rosalin Bonetta and Gianluca Valentino. Machine learning techniques for protein function prediction. *Proteins: Structure, Function, and Bioinformatics*, 88(3):397–413, 2020.

- Avishek Joey Bose, Tara Akhound-Sadegh, Kilian Fatras, Guillaume Huguet, Jarrid Rector-Brooks, Cheng-Hao Liu, Andrei Cristian Nica, Maksym Korablyov, Michael Bronstein, and Alexander Tong. Se (3)-stochastic flow matching for protein backbone generation. *arXiv preprint arXiv:2310.02391*, 2023.
- Martin Buttenschoen, Garrett M Morris, and Charlotte M Deane. Posebusters: Ai-based docking methods fail to generate physically valid poses or generalise to novel sequences. *Chemical Science*, 15(9):3130–3139, 2024.
- Andrew Campbell, Joe Benton, Valentin De Bortoli, Thomas Rainforth, George Deligiannidis, and Arnaud Doucet. A continuous time framework for discrete denoising models. *Advances in Neural Information Processing Systems*, 35:28266–28279, 2022.
- Andrew Campbell, Jason Yim, Regina Barzilay, Tom Rainforth, and Tommi Jaakkola. Generative flows on discrete state-spaces: Enabling multimodal flows with applications to protein co-design. *arXiv preprint arXiv:2402.04997*, 2024.
- Eleanor Campbell, Miriam Kaltenbach, Galen J Correy, Paul D Carr, Benjamin T Porebski, Emma K Livingstone, Livnat Afriat-Jurnou, Ashley M Buckle, Martin Weik, Florian Hollfelder, et al. The role of protein dynamics in the evolution of new enzyme function. *Nature chemical biology*, 12(11):944–950, 2016.
- Ron Caspi, Richard Billington, Ingrid M Keseler, Anamika Kothari, Markus Krummenacker, Peter E Midford, Wai Kit Ong, Suzanne Paley, Pallavi Subhraveti, and Peter D Karp. The metacyc database of metabolic pathways and enzymes—a 2019 update. *Nucleic acids research*, 48(D1):D445–D453, 2020.
- Chai Discovery. Chai-1: Decoding the molecular interactions of life. *bioRxiv*, 2024. doi: 10.1101/2024.10.10.615955. URL <https://www.biorxiv.org/content/early/2024/10/11/2024.10.10.615955>.
- Alexander E Chu, Jinho Kim, Lucy Cheng, Gina El Nesr, Minkai Xu, Richard W Shuai, and Po-Ssu Huang. An all-atom protein generative model. *Proceedings of the National Academy of Sciences*, 121(27):e2311500121, 2024.
- Daniela Concolino, Federica Deodato, and Rossella Parini. Enzyme replacement therapy: efficacy and limitations. *Italian journal of pediatrics*, 44:117–126, 2018.
- Gene Ontology Consortium. The gene ontology (go) database and informatics resource. *Nucleic acids research*, 32(suppl\_1):D258–D261, 2004.
- Robert A Copeland. *Enzymes: a practical introduction to structure, mechanism, and data analysis*. John Wiley & Sons, 2023.
- Athel Cornish-Bowden. *Fundamentals of enzyme kinetics*. John Wiley & Sons, 2013.
- Justas Dauparas, Ivan Anishchenko, Nathaniel Bennett, Hua Bai, Robert J Ragotte, Lukas F Milles, Basile IM Wicky, Alexis Courbet, Rob J de Haas, Neville Bethel, et al. Robust deep learning-based protein sequence design using proteinmpnn. *Science*, 378(6615):49–56, 2022.
- Justas Dauparas, Gyu Rie Lee, Robert Pecoraro, Linna An, Ivan Anishchenko, Cameron Glasscock, and David Baker. Atomic context-conditioned protein sequence design using ligandmpnn. *Biorxiv*, pp. 2023–12, 2023.
- Mark A DePristo, Daniel M Weinreich, and Daniel L Hartl. Missense meanderings in sequence space: a biophysical view of protein evolution. *Nature Reviews Genetics*, 6(9):678–687, 2005.
- Jacob Devlin. Bert: Pre-training of deep bidirectional transformers for language understanding. *arXiv preprint arXiv:1810.04805*, 2018.
- Enrico Di Cera. Serine proteases. *IUBMB life*, 61(5):510–515, 2009.
- Vincent GH Eijsink, Sigrid Gåseidnes, Torben V Borchert, and Bertus Van Den Burg. Directed evolution of enzyme stability. *Biomolecular engineering*, 22(1-3):21–30, 2005.

- Ahmed Elnaggar, Michael Heinzinger, Christian Dallago, Ghaliya Rehawi, Yu Wang, Llion Jones, Tom Gibbs, Tamas Feher, Christoph Angerer, Martin Steinegger, et al. Prottrans: Toward understanding the language of life through self-supervised learning. *IEEE transactions on pattern analysis and machine intelligence*, 44(10):7112–7127, 2021.
- Richard Evans, Michael O’Neill, Alexander Pritzel, Natasha Antropova, Andrew Senior, Tim Green, Augustin Židek, Russ Bates, Sam Blackwell, Jason Yim, et al. Protein complex prediction with alphafold-multimer. *bioRxiv*, pp. 2021–10, 2021.
- J-L Ferrer, MB Austin, C Stewart Jr, and JP Noel. Structure and function of enzymes involved in the biosynthesis of phenylpropanoids. *Plant Physiology and Biochemistry*, 46(3):356–370, 2008.
- Japheth E Gado, Matthew Knotts, Ada Y Shaw, Debora Marks, Nicholas P Gauthier, Chris Sander, and Gregg T Beckham. Deep learning prediction of enzyme optimum ph. *bioRxiv*, pp. 2023–06, 2023.
- Zhangyang Gao, Cheng Tan, Pablo Chacón, and Stan Z Li. Pifold: Toward effective and efficient protein inverse folding. *arXiv preprint arXiv:2209.12643*, 2022.
- Hazel M Girvan and Andrew W Munro. Applications of microbial cytochrome p450 enzymes in biotechnology and synthetic biology. *Current opinion in chemical biology*, 31:136–145, 2016.
- Margaret E Glasner, John A Gerlt, and Patricia C Babbitt. Evolution of enzyme superfamilies. *Current opinion in chemical biology*, 10(5):492–497, 2006.
- Vladimir Gligorijević, P Douglas Renfrew, Tomasz Kosciolk, Julia Koehler Leman, Daniel Berenberg, Tommi Vatanen, Chris Chandler, Bryn C Taylor, Ian M Fisk, Hera Vlamakis, et al. Structure-based protein function prediction using graph convolutional networks. *Nature communications*, 12(1):3168, 2021.
- Tomas Hayes, Roshan Rao, Halil Akin, Nicholas J Sofroniew, Deniz Oktay, Zeming Lin, Robert Verkuil, Vincent Q Tran, Jonathan Deaton, Marius Wiggert, et al. Simulating 500 million years of evolution with a language model. *bioRxiv*, pp. 2024–07, 2024.
- Reinhart Heinrich and Stefan Schuster. *The regulation of cellular systems*. Springer Science & Business Media, 2012.
- Maarten L Hekkelman, Ida de Vries, Robbie P Joosten, and Anastassis Perrakis. Alphafill: enriching alphafold models with ligands and cofactors. *Nature Methods*, 20(2):205–213, 2023.
- C Eric Hodgman and Michael C Jewett. Cell-free synthetic biology: thinking outside the cell. *Metabolic engineering*, 14(3):261–269, 2012.
- Euan J Hossack, Florence J Hardy, and Anthony P Green. Building enzymes through design and evolution. *ACS Catalysis*, 13(19):12436–12444, 2023.
- Jeremy Howard and Sebastian Ruder. Universal language model fine-tuning for text classification. *arXiv preprint arXiv:1801.06146*, 2018.
- Chenqing Hua, Sitao Luan, Qian Zhang, and Jie Fu. Graph neural networks intersect probabilistic graphical models: A survey. *arXiv preprint arXiv:2206.06089*, 2022a.
- Chenqing Hua, Guillaume Rabusseau, and Jian Tang. High-order pooling for graph neural networks with tensor decomposition. *Advances in Neural Information Processing Systems*, 35:6021–6033, 2022b.
- Chenqing Hua, Sitao Luan, Minkai Xu, Rex Ying, Jie Fu, Stefano Ermon, and Doina Precup. Mudiff: Unified diffusion for complete molecule generation. *arXiv preprint arXiv:2304.14621*, 2023.
- Chenqing Hua, Connor Coley, Guy Wolf, Doina Precup, and Shuangjia Zheng. Effective protein-protein interaction exploration with ppi retrieval. *arXiv preprint arXiv:2402.03675*, 2024a.
- Chenqing Hua, Yong Liu, Dinghuai Zhang, Odin Zhang, Sitao Luan, Kevin K Yang, Guy Wolf, Doina Precup, and Shuangjia Zheng. Enzymeflow: Generating reaction-specific enzyme catalytic pockets through flow matching and co-evolutionary dynamics. *arXiv preprint arXiv:2410.00327*, 2024b.



- Chenqing Hua, Bozitao Zhong, Sitao Luan, Liang Hong, Guy Wolf, Doina Precup, and Shuangjia Zheng. Reactzyme: A benchmark for enzyme-reaction prediction. *arXiv preprint arXiv:2408.13659*, 2024c.
- Jaime Huerta-Cepas, Damian Szklarczyk, Davide Heller, Ana Hernández-Plaza, Sofia K Forslund, Helen Cook, Daniel R Mende, Ivica Letunic, Thomas Rattei, Lars J Jensen, et al. eggNOG 5.0: a hierarchical, functionally and phylogenetically annotated orthology resource based on 5090 organisms and 2502 viruses. *Nucleic acids research*, 47(D1):D309–D314, 2019.
- John B Ingraham, Max Baranov, Zak Costello, Karl W Barber, Wujie Wang, Ahmed Ismail, Vincent Frappier, Dana M Lord, Christopher Ng-Thow-Hing, Erik R Van Vlack, et al. Illuminating protein space with a programmable generative model. *Nature*, 623(7989):1070–1078, 2023.
- Clemens Isert, Kenneth Atz, and Gisbert Schneider. Structure-based drug design with geometric deep learning. *Current Opinion in Structural Biology*, 79:102548, 2023.
- Christian Jäckel, Peter Kast, and Donald Hilvert. Protein design by directed evolution. *Annu. Rev. Biophys.*, 37(1):153–173, 2008.
- Roy A Jensen. Enzyme recruitment in evolution of new function. *Annual review of microbiology*, 30(1):409–425, 1976.
- John Jumper, Richard Evans, Alexander Pritzel, Tim Green, Michael Figurnov, Olaf Ronneberger, Kathryn Tunyasuvunakool, Russ Bates, Augustin Žídek, Anna Potapenko, et al. Highly accurate protein structure prediction with alphafold. *Nature*, 596(7873):583–589, 2021.
- Jay D Keasling. Manufacturing molecules through metabolic engineering. *Science*, 330(6009):1355–1358, 2010.
- Brianne R King, Kiera H Sumida, Jessica L Caruso, David Baker, and Jesse G Zalatan. Computational stabilization of a non-heme iron enzyme enables efficient evolution of new function. *bioRxiv*, pp. 2024–04, 2024.
- Joseph Kraut. How do enzymes work? *Science*, 242(4878):533–540, 1988.
- Rohith Krishna, Jue Wang, Woody Ahern, Pascal Sturmfels, Preetham Venkatesh, Indrek Kalvet, Gyu Rie Lee, Felix S Morey-Burrows, Ivan Anishchenko, Ian R Humphreys, et al. Generalized biomolecular modeling and design with rosettafold all-atom. *Science*, 384(6693):ead12528, 2024.
- Alexander Kroll, Sahasra Ranjan, Martin KM Engqvist, and Martin J Lercher. A general model to predict small molecule substrates of enzymes based on machine and deep learning. *Nature communications*, 14(1):2787, 2023.
- Maxat Kulmanov and Robert Hoehndorf. Deepgoplus: improved protein function prediction from sequence. *Bioinformatics*, 36(2):422–429, 2020.
- Robert Langer and David A Tirrell. Designing materials for biology and medicine. *Nature*, 428(6982):487–492, 2004.
- Yeqing Lin and Mohammed AlQuraishi. Generating novel, designable, and diverse protein structures by equivariantly diffusing oriented residue clouds. *arXiv preprint arXiv:2301.12485*, 2023.
- Yeqing Lin, Minji Lee, Zhao Zhang, and Mohammed AlQuraishi. Out of many, one: Designing and scaffolding proteins at the scale of the structural universe with genie 2. *arXiv preprint arXiv:2405.15489*, 2024.
- Zeming Lin, Halil Akin, Roshan Rao, Brian Hie, Zhongkai Zhu, Wenting Lu, Allan dos Santos Costa, Maryam Fazel-Zarandi, Tom Sercu, Sal Candido, et al. Language models of protein sequences at the scale of evolution enable accurate structure prediction. *BioRxiv*, 2022:500902, 2022.
- Yaron Lipman, Ricky TQ Chen, Heli Ben-Hamu, Maximilian Nickel, and Matt Le. Flow matching for generative modeling. *arXiv preprint arXiv:2210.02747*, 2022.

- Dina Listov, Casper A Goverde, Bruno E Correia, and Sarel Jacob Fleishman. Opportunities and challenges in design and optimization of protein function. *Nature Reviews Molecular Cell Biology*, pp. 1–15, 2024.
- Wenfang Liu and Ping Wang. Cofactor regeneration for sustainable enzymatic biosynthesis. *Biotechnology advances*, 25(4):369–384, 2007.
- Aaron Lou, Chenlin Meng, and Stefano Ermon. Discrete diffusion language modeling by estimating the ratios of the data distribution. *arXiv preprint arXiv:2310.16834*, 2023.
- Jiarui Lu, Xiaoyin Chen, Stephen Zhewen Lu, Chence Shi, Hongyu Guo, Yoshua Bengio, and Jian Tang. Structure language models for protein conformation generation. *arXiv preprint arXiv:2410.18403*, 2024.
- Sitao Luan, Mingde Zhao, Chenqing Hua, Xiao-Wen Chang, and Doina Precup. Complete the missing half: Augmenting aggregation filtering with diversification for graph convolutional networks. *arXiv preprint arXiv:2008.08844*, 2020.
- Sitao Luan, Chenqing Hua, Qincheng Lu, Jiaqi Zhu, Mingde Zhao, Shuyuan Zhang, Xiao-Wen Chang, and Doina Precup. Revisiting heterophily for graph neural networks. *Advances in neural information processing systems*, 35:1362–1375, 2022.
- Sitao Luan, Chenqing Hua, Qincheng Lu, Liheng Ma, Lirong Wu, Xinyu Wang, Minkai Xu, Xiao-Wen Chang, Doina Precup, Rex Ying, et al. The heterophilic graph learning handbook: Benchmarks, models, theoretical analysis, applications and challenges. *arXiv preprint arXiv:2407.09618*, 2024a.
- Sitao Luan, Chenqing Hua, Minkai Xu, Qincheng Lu, Jiaqi Zhu, Xiao-Wen Chang, Jie Fu, Jure Leskovec, and Doina Precup. When do graph neural networks help with node classification? Investigating the homophily principle on node distinguishability. *Advances in Neural Information Processing Systems*, 36, 2024b.
- Xizeng Mao, Tao Cai, John G Olyarchuk, and Liping Wei. Automated genome annotation and pathway identification using the kegg orthology (ko) as a controlled vocabulary. *Bioinformatics*, 21(19):3787–3793, 2005.
- Peter G Mikhael, Itamar Chinn, and Regina Barzilay. Clipzyme: Reaction-conditioned virtual screening of enzymes. *arXiv preprint arXiv:2402.06748*, 2024.
- Milot Mirdita, Konstantin Schütze, Yoshitaka Moriwaki, Lim Heo, Sergey Ovchinnikov, and Martin Steinegger. Colabfold: making protein folding accessible to all. *Nature methods*, 19(6):679–682, 2022.
- Geraldene Munsamy, Sebastian Lindner, Philipp Lorenz, and Noelia Ferruz. Zymctrl: a conditional language model for the controllable generation of artificial enzymes. In *NeurIPS Machine Learning in Structural Biology Workshop*, 2022.
- Yukito Murakami, Jun-ichi Kikuchi, Yoshio Hisaeda, and Osamu Hayashida. Artificial enzymes. *Chemical reviews*, 96(2):721–758, 1996.
- Kwangho Nam, Yihan Shao, Dan T Major, and Magnus Wolf-Watz. Perspectives on computational enzyme modeling: From mechanisms to design and drug development. *ACS omega*, 9(7):7393–7412, 2024.
- Jens Nielsen and Jay D Keasling. Engineering cellular metabolism. *Cell*, 164(6):1185–1197, 2016.
- Pascal Notin, Aaron Kollasch, Daniel Ritter, Lood Van Niekerk, Steffanie Paul, Han Spinner, Nathan Rollins, Ada Shaw, Rose Orenbuch, Ruben Weitzman, et al. Proteingym: Large-scale benchmarks for protein fitness prediction and design. *Advances in Neural Information Processing Systems*, 36, 2024.
- Jeffrey Ouyang-Zhang, Daniel Diaz, Adam Klivans, and Philipp Krähenbühl. Predicting a protein’s stability under a million mutations. *Advances in Neural Information Processing Systems*, 36, 2024.

- Martin Pacesa, Lennart Nickel, Joseph Schmidt, Ekaterina Pyatova, Christian Schellhaas, Lucas Kissling, Ana Alcaraz-Serna, Yehlin Cho, Kourosh H Ghamary, Laura Vinue, et al. Bindcraft: one-shot design of functional protein binders. *bioRxiv*, pp. 2024–09, 2024.
- Csaba Pál, Balázs Papp, and Martin J Lercher. An integrated view of protein evolution. *Nature reviews genetics*, 7(5):337–348, 2006.
- Gaspar P Pinto, Marina Corbella, Andrey O Demkiv, and Shina Caroline Lynn Kamerlin. Exploiting enzyme evolution for computational protein design. *Trends in Biochemical Sciences*, 47(5): 375–389, 2022.
- Alec Radford, Jong Wook Kim, Chris Hallacy, Aditya Ramesh, Gabriel Goh, Sandhini Agarwal, Girish Sastry, Amanda Askell, Pamela Mishkin, Jack Clark, et al. Learning transferable visual models from natural language supervision. In *International conference on machine learning*, pp. 8748–8763. PMLR, 2021.
- Manfred T Reetz, Ge Qu, and Zhoutong Sun. Engineered enzymes for the synthesis of pharmaceuticals and other high-value products. *Nature Synthesis*, 3(1):19–32, 2024.
- Peter K Robinson. Enzymes: principles and biotechnological applications. *Essays in biochemistry*, 59:1, 2015.
- Philip A Romero and Frances H Arnold. Exploring protein fitness landscapes by directed evolution. *Nature reviews Molecular cell biology*, 10(12):866–876, 2009.
- Jae Yong Ryu, Hyun Uk Kim, and Sang Yup Lee. Deep learning enables high-quality and high-throughput prediction of enzyme commission numbers. *Proceedings of the National Academy of Sciences*, 116(28):13996–14001, 2019.
- Subham Sekhar Sahoo, Marianne Arriola, Yair Schiff, Aaron Gokaslan, Edgar Marroquin, Justin T Chiu, Alexander Rush, and Volodymyr Kuleshov. Simple and effective masked diffusion language models. *arXiv preprint arXiv:2406.07524*, 2024.
- Victor Garcia Satorras, Emiel Hoogeboom, and Max Welling. E (n) equivariant graph neural networks. In *International conference on machine learning*, pp. 9323–9332. PMLR, 2021.
- Claudia Schmidt-Dannert and Frances H Arnold. Directed evolution of industrial enzymes. *Trends in biotechnology*, 17(4):135–136, 1999.
- Ida Schomburg, Antje Chang, Oliver Hofmann, Christian Ebeling, Frank Ehrentreich, and Dietmar Schomburg. Brenda: a resource for enzyme data and metabolic information. *Trends in biochemical sciences*, 27(1):54–56, 2002.
- Andrew W Senior, Richard Evans, John Jumper, James Kirkpatrick, Laurent Sifre, Tim Green, Chongli Qin, Augustin Židek, Alexander WR Nelson, Alex Bridgland, et al. Improved protein structure prediction using potentials from deep learning. *Nature*, 577(7792):706–710, 2020.
- Jiaxin Shi, Kehang Han, Zhe Wang, Arnaud Doucet, and Michalis K Titsias. Simplified and generalized masked diffusion for discrete data. *arXiv preprint arXiv:2406.04329*, 2024.
- Ian Sillitoe, Nicola Bordin, Natalie Dawson, Vaishali P Waman, Paul Ashford, Harry M Scholes, Camilla SM Pang, Laurel Woodridge, Clemens Rauer, Neeladri Sen, et al. Cath: increased structural coverage of functional space. *Nucleic acids research*, 49(D1):D266–D273, 2021.
- Yang Song, Jascha Sohl-Dickstein, Diederik P Kingma, Abhishek Kumar, Stefano Ermon, and Ben Poole. Score-based generative modeling through stochastic differential equations. *arXiv preprint arXiv:2011.13456*, 2020.
- Misha Soskine and Dan S Tawfik. Mutational effects and the evolution of new protein functions. *Nature Reviews Genetics*, 11(8):572–582, 2010.
- Martin Steinegger and Johannes Söding. Mmseqs2 enables sensitive protein sequence searching for the analysis of massive data sets. *Nature biotechnology*, 35(11):1026–1028, 2017.

- Haoran Sun, Lijun Yu, Bo Dai, Dale Schuurmans, and Hanjun Dai. Score-based continuous-time discrete diffusion models. *arXiv preprint arXiv:2211.16750*, 2022.
- Hugo Touvron, Louis Martin, Kevin Stone, Peter Albert, Amjad Almahairi, Yasmine Babaei, Nikolay Bashlykov, Soumya Batra, Prajjwal Bhargava, Shruti Bhosale, et al. Llama 2: Open foundation and fine-tuned chat models. *arXiv preprint arXiv:2307.09288*, 2023.
- Oleg Trott and Arthur J Olson. Autodock vina: improving the speed and accuracy of docking with a new scoring function, efficient optimization, and multithreading. *Journal of computational chemistry*, 31(2):455–461, 2010.
- Jérôme Tubiana, Dina Schneidman-Duhovny, and Haim J Wolfson. Scannet: an interpretable geometric deep learning model for structure-based protein binding site prediction. *Nature Methods*, 19(6):730–739, 2022.
- Michel van Kempen, Stephanie S Kim, Charlotte Tumescheit, Milot Mirdita, Cameron LM Gilchrist, Johannes Söding, and Martin Steinegger. Foldseek: fast and accurate protein structure search. *Biorxiv*, pp. 2022–02, 2022.
- Jue Wang, Sidney Lisanza, David Juergens, Doug Tischer, Joseph L Watson, Karla M Castro, Robert Ragotte, Amijai Saragovi, Lukas F Milles, Minkyung Baek, et al. Scaffolding protein functional sites using deep learning. *Science*, 377(6604):387–394, 2022.
- Joseph L Watson, David Juergens, Nathaniel R Bennett, Brian L Trippe, Jason Yim, Helen E Eisenach, Woody Ahern, Andrew J Borst, Robert J Ragotte, Lukas F Milles, et al. De novo design of protein structure and function with rfdiffusion. *Nature*, 620(7976):1089–1100, 2023.
- David Whitford. *Proteins: structure and function*. John Wiley & Sons, 2013.
- GN Wilkinson. Statistical estimations in enzyme kinetics. *Biochemical Journal*, 80(2):324, 1961.
- Kevin E Wu, Kevin K Yang, Rianne van den Berg, Sarah Alamdari, James Y Zou, Alex X Lu, and Ava P Amini. Protein structure generation via folding diffusion. *Nature communications*, 15(1): 1059, 2024.
- Yu Xia and Michael Levitt. Simulating protein evolution in sequence and structure space. *Current Opinion in Structural Biology*, 14(2):202–207, 2004.
- Jason Yang, Aadyot Bhatnagar, Jeffrey A Ruffolo, and Ali Madani. Conditional enzyme generation using protein language models with adapters. *arXiv preprint arXiv:2410.03634*, 2024a.
- Jason Yang, Ariane Mora, Shengchao Liu, Bruce J Wittmann, Anima Anandkumar, Frances H Arnold, and Yisong Yue. Care: a benchmark suite for the classification and retrieval of enzymes. *arXiv preprint arXiv:2406.15669*, 2024b.
- Kevin K Yang, Zachary Wu, and Frances H Arnold. Machine-learning-guided directed evolution for protein engineering. *Nature methods*, 16(8):687–694, 2019.
- Jason Yim, Andrew Campbell, Andrew YK Foong, Michael Gastegger, José Jiménez-Luna, Sarah Lewis, Victor Garcia Satorras, Bastiaan S Veeling, Regina Barzilay, Tommi Jaakkola, et al. Fast protein backbone generation with se (3) flow matching. *arXiv preprint arXiv:2310.05297*, 2023a.
- Jason Yim, Brian L Trippe, Valentin De Bortoli, Emile Mathieu, Arnaud Doucet, Regina Barzilay, and Tommi Jaakkola. Se (3) diffusion model with application to protein backbone generation. *arXiv preprint arXiv:2302.02277*, 2023b.
- Han Yu, Huaxiang Deng, Jiahui He, Jay D Keasling, and Xiaozhou Luo. Unikp: a unified framework for the prediction of enzyme kinetic parameters. *Nature communications*, 14(1):8211, 2023a.
- Mengyao Yu, Yundian Zeng, Mingyang Wang, Chenqing Hua, Sunliang Cui, Peichen Pan, Chang-Yu Hsieh, Tingjun Hou, Odin Zhang, Yufei Huang, et al. Fragger: Towards 3d geometry reliable fragment-based molecular generation. *Chemical Science*, 2024.
- Tianhao Yu, Haiyang Cui, Jianan Canal Li, Yunan Luo, Guangde Jiang, and Huimin Zhao. Enzyme function prediction using contrastive learning. *Science*, 379(6639):1358–1363, 2023b.

- Vinicius Zambaldi, David La, Alexander E Chu, Harshnira Patani, Amy E Danson, Tristan OC Kwan, Thomas Frerix, Rosalia G Schneider, David Saxton, Ashok Thillaisundaram, et al. De novo design of high-affinity protein binders with alphaproteo. *arXiv preprint arXiv:2409.08022*, 2024.
- Odin Zhang, Yufei Huang, Shichen Cheng, Mengyao Yu, Xujun Zhang, Haitao Lin, Yundian Zeng, Mingyang Wang, Zhenxing Wu, Huifeng Zhao, et al. Deep geometry handling and fragment-wise molecular 3d graph generation. *arXiv preprint arXiv:2404.00014*, 2024a.
- Odin Zhang, Jieyu Jin, Haitao Lin, Jintu Zhang, Chenqing Hua, Yufei Huang, Huifeng Zhao, Chang-Yu Hsieh, and Tingjun Hou. Ecloudgen: Access to broader chemical space for structure-based molecule generation. *bioRxiv*, pp. 2024–06, 2024b.
- Yang Zhang and Jeffrey Skolnick. Tm-align: a protein structure alignment algorithm based on the tm-score. *Nucleic acids research*, 33(7):2302–2309, 2005.
- Zaixi Zhang, Zepu Lu, Hao Zhongkai, Marinka Zitnik, and Qi Liu. Full-atom protein pocket design via iterative refinement. *Advances in Neural Information Processing Systems*, 36:16816–16836, 2023.
- Zaixi Zhang, Wanxiang Shen, Qi Liu, and Marinka Zitnik. Pocketgen: Generating full-atom ligand-binding protein pockets. *bioRxiv*, pp. 2024–02, 2024c.
- Zaixi Zhang, Marinka Zitnik, and Qi Liu. Generalized protein pocket generation with prior-informed flow matching. *arXiv preprint arXiv:2409.19520*, 2024d.
- Zuobai Zhang, Minghao Xu, Arian Jamasb, Vijil Chenthamarakshan, Aurelie Lozano, Payel Das, and Jian Tang. Protein representation learning by geometric structure pretraining. *arXiv preprint arXiv:2203.06125*, 2022.
- Lingxiao Zhao, Xueying Ding, Lijun Yu, and Leman Akoglu. Improving and unifying discrete and continuous-time discrete denoising diffusion. *arXiv preprint arXiv:2402.03701*, 2024.
- Lin Zheng, Jianbo Yuan, Lei Yu, and Lingpeng Kong. A reparameterized discrete diffusion model for text generation. *arXiv preprint arXiv:2302.05737*, 2023.
- Emile Zuckerkandl and Linus Pauling. Molecules as documents of evolutionary history. *Journal of theoretical biology*, 8(2):357–366, 1965.

## A EXTENDED RELATED WORK

### A.1 PROTEIN EVOLUTION

Protein evolution learns how proteins change over time through processes such as mutation, selection, and genetic drift (Pál et al., 2006; Bloom & Arnold, 2009), which influence protein functions. Studies on protein evolution focus on understanding the molecular mechanisms driving changes in protein sequences and structures. Zuckerkandl & Pauling (1965) introduce the concept of the molecular clock, which postulates that proteins evolve at a relatively constant rate over time, providing a framework for estimating divergence times between species. DePristo et al. (2005) show that evolutionary rates are influenced by functional constraints, with regions critical to protein function (*e.g.*, active sites, binding interfaces) evolving more slowly due to purifying selection. This understanding leads to the development of methods for detecting functionally important residues based on evolutionary conservation. Understanding protein evolution has practical applications in protein engineering. By studying how natural proteins evolve to acquire new functions, researchers design synthetic proteins with desired properties (Xia & Levitt, 2004; Jäckel et al., 2008). Additionally, deep learning models increasingly integrate evolutionary principles to predict protein function and stability, design novel enzymes, and guide protein engineering (Yang et al., 2019; AlQuraishi, 2019; Jumper et al., 2021).

### A.2 PROTEIN REPRESENTATION LEARNING

Graph representation learning emerges as a potent strategy for learning about proteins and molecules, focusing on structured, non-Euclidean data (Satorras et al., 2021; Luan et al., 2020; 2022; Hua et al., 2022a;b; Luan et al., 2024b;a). In this context, proteins and molecules can be effectively modeled as 2D graphs or 3D point clouds, where nodes correspond to individual atoms or residues, and edges represent interactions between them (Gligorijević et al., 2021; Zhang et al., 2022; Hua et al., 2023; Zhang et al., 2024a). Indeed, representing proteins and molecules as graphs or point clouds offers a valuable approach for gaining insights into and learning the fundamental geometric and chemical mechanisms governing protein-ligand interactions. This representation allows for a more comprehensive exploration of the intricate relationships and structural features within protein-ligand structures (Tubiana et al., 2022; Isert et al., 2023; Zhang et al., 2024b; Yu et al., 2024).

### A.3 PROTEIN FUNCTION ANNOTATION

Protein function prediction aims to determine the biological role of a protein based on its sequence, structure, or other features. It is a crucial task in bioinformatics, often leveraging databases such as Gene Ontology (GO), Enzyme Commission (EC) numbers, and KEGG Orthology (KO) annotations (Bairoch, 2000; Consortium, 2004; Mao et al., 2005). Traditional methods like BLAST, PSI-BLAST, and eggNOG infer function by comparing sequence alignments and similarities (Altschul et al., 1990; 1997; Huerta-Cepas et al., 2019). Recently, deep learning has introduced more advanced approaches for protein function prediction (Ryu et al., 2019; Kulmanov & Hoehndorf, 2020; Bonetta & Valentino, 2020). There are two major types of function prediction models, one uses only protein sequence as their input, while the other also uses experimentally-determined or predicted protein structure as input. Typically, these methods predict EC or GO annotations to approximate protein functions, rather than describing the exact catalyzed reaction, which is a limitation of these approaches.

### A.4 GENERATIVE MODELS FOR PROTEIN AND POCKET DESIGN

Recent advancements in generative models have advanced the field of protein design and binding pocket design, enabling the creation of proteins or binding pockets with desired properties and functions (Yim et al., 2023a;b; Chu et al., 2024; Hua et al., 2024a; Abramson et al., 2024). For example, RFDiffusion (Watson et al., 2023) employs denoising diffusion in conjunction with RoseTTAFold (Baek et al., 2021) for *de novo* protein structure design, achieving wet-lab-level generated structures that can be extended to binding pocket design. RFDiffusionAA (Krishna et al., 2024) extends RFDiffusion for joint modeling of protein and ligand structures, generating ligand-binding proteins and further leveraging MPNNs for sequence design. Additionally, FAIR (Zhang et al., 2023) and PocketGen (Zhang et al., 2024c) use a two-stage coarse-to-fine refinement approach to co-design pocket structures and sequences. Recent models leveraging flow matching frameworks have shown

promising results in these tasks. For instance, FoldFlow (Bose et al., 2023) introduces a series of flow models for protein backbone design, improving training stability and efficiency. FrameFlow (Yim et al., 2023a) further enhances sampling efficiency and demonstrates success in motif-scaffolding tasks using flow matching, while MultiFlow (Campbell et al., 2024) advances to structure and sequence co-design. These flow models, initially applied to protein backbones, have been further generalized to binding pockets. For example, PocketFlow (Zhang et al., 2024d) combines flow matching with physical priors to explicitly learn protein-ligand interactions in binding pocket design, achieving stronger results compared to RFDiffusionAA. And EnzymeFlow (Hua et al., 2024b) introduces a flow-based generative model, leveraging enzyme-reaction co-evolution and structure-based pre-training for enzyme catalytic pocket generation.

**GENZYME Contributions.** The first major contribution of GENZYME is its ability to perform *de novo* enzyme design, generating catalytic pocket structures and full enzyme structures capable of catalyzing previously unseen reactions. The second contribution is GENZYME generation of synthetic enzyme-substrate binding complex data, which aids in a deeper understanding of enzyme-substrate interactions and metabolic processes. The third contribution is the fine-tuned protein language models for enzyme representation learning, optimizing them for enzyme-specific tasks such as catalytic pocket inpainting, enzyme inverse folding, and enzyme representation learning.

## B PRELIMINARIES

### B.1 ENZYME-REACTION NOTATIONS

Following Jumper et al. (2021); Yim et al. (2023a), we refer to the enzyme structure as the backbone atomic coordinates of each residue. An enzyme with number of residues  $N_E$  can be parameterized into SE(3) residue frames  $\{(x_i, r_i, a_i)\}_{i=1}^{N_E}$ , where  $x_i \in \mathbb{R}^3$  represents the position (translation) of the  $C_\alpha$  atom of the  $i$ -th residue,  $r_i \in \text{SO}(3)$  is a rotation matrix defining the local frame relative to a global reference frame, and  $a_i \in \{1, \dots, 20\}$  denotes the amino acid type. We refer to the residue block as  $E_i = (x_i, r_i, a_i)$ , and the entire enzyme is described by a set of residues  $\mathbf{E} = \{E_i\}_{i=1}^{N_E}$ .

A chemical reaction,  $m_r: m_1 \xrightarrow{\mathbf{E}} m_2$ , describes a process in which a substrate molecule  $m_1$  is transformed into a product molecule  $m_2$ , catalyzed by the enzyme  $\mathbf{E}$ . The reaction, substrate, and product can be represented by canonical SMILES. The catalytic pocket  $\mathbf{E}^P = \{E_i^P\}_{i=1}^{N_P}$ , consisting of  $N_P$  residues, is the active site within the enzyme  $\mathbf{E}$  where the substrate  $m_1$  binds, forming an enzyme-substrate complex  $\mathbf{C} = [\mathbf{E}, m_1]$ , facilitating the reaction. Additionally, the enzyme scaffold  $\mathbf{E}^S = \{E_i^S\}_{i=1}^{N_S}$ , consisting of  $N_S$  residues, complements the catalytic pocket, such that  $\mathbf{E} = \mathbf{E}^P \cup \mathbf{E}^S$  where  $N_E = N_P + N_S$ .

### B.2 CONDITIONAL FLOW MATCHING

Flow matching describes a process where a flow transforms a simple distribution  $p_0$  into the target data distribution  $p_1$  (Lipman et al., 2022). The goal in flow matching is to train a neural network  $v_\theta(\epsilon_t, t)$  that approximates the vector field  $u_t(\epsilon)$ , which measures the transformation of the distribution  $p_t(\epsilon_t)$  as it evolves toward  $p_1(\epsilon_t)$  over time  $t \in [0, 1)$ . The process is optimized using a regression loss defined as  $\mathcal{L}_{\text{FM}} = \mathbb{E}_{t \sim \mathcal{U}[0,1], p_t(\epsilon_t)} \|v_\theta(\epsilon_t, t) - u_t(\epsilon)\|^2$ . However, directly computing  $u_t(\epsilon)$  is often intractable in practice. Instead, a conditional vector field  $u_t(\epsilon|\epsilon_1)$  is defined, and the conditional flow matching objective is computed as  $\mathcal{L}_{\text{CFM}} = \mathbb{E}_{t \sim \mathcal{U}[0,1], p_t(\epsilon_t)} \|v_\theta(\epsilon_t, t) - u_t(\epsilon|\epsilon_1)\|^2$ . Notably,  $\nabla_\theta \mathcal{L}_{\text{FM}} = \nabla_\theta \mathcal{L}_{\text{CFM}}$ .

During inference or sampling, an ODEsolver, *e.g.*, Euler method, is typically used to solve the ODE governing the flow, expressed as  $\epsilon_1 = \text{ODEsolver}(\epsilon_0, v_\theta, 0, 1)$ , where  $\epsilon_0$  is the initial data and  $\epsilon_1$  is the generated data. In actual training, rather than directly predicting the vector fields, it is more common to use the neural network to predict the final state at  $t = 1$ , then interpolates to calculate the vector fields. This approach has been shown to be more efficient and effective for network optimization (Yim et al., 2023a; Bose et al., 2023; Campbell et al., 2024).

### B.2.1 CONTINUOUS VARIABLE TRAJECTORY

Given the predictions for translation  $\hat{x}_1$  and rotation  $\hat{r}_1$  at  $t = 1$ , we can interpolate and their corresponding vector fields are computed as follows:

$$v_\theta(x_t, t) = \frac{\hat{x}_1 - x_t}{1 - t}, \quad v_\theta(r_t, t) = \frac{\log_{r_t} \hat{r}_1}{1 - t}. \quad (2)$$

The sampling or trajectory can then be computed using Euler steps with a step size  $\Delta t$ , as follows:

$$x_{t+\Delta t} = x_t + v_\theta(x_t, t) \cdot \Delta t, \quad r_{t+\Delta t} = r_t + v_\theta(r_t, t) \cdot \Delta t, \quad (3)$$

where the prior of  $x_0, r_0$  are chosen as the uniform distribution on  $\mathbb{R}^3$  and  $\text{SO}(3)$ , respectively.

### B.2.2 DISCRETE VARIABLE TRAJECTORY

For the discrete variables, we use continuous time Markov chains (CTMC).

**Continuous Time Markov Chain.** A sequence trajectory  $\epsilon_t$  over time  $t \in [0, 1]$  that follows a CTMC alternates between resting in its current state and periodically jumping to another randomly chosen state. The frequency and destination of the jumps are determined by the rate matrix  $R_t \in \mathbb{R}^{N \times N}$  with the constraint its off-diagonal elements are non-negative. The probability of  $\epsilon_t$  jumping to a different state  $s$  follows  $R_t(\epsilon_t, s)dt$  for the next infinitesimal time step  $dt$ . We can express the transition probability as

$$p_{t+dt}(s|\epsilon_t) = \delta\{\epsilon_t, s\} + R_t(\epsilon_t, s)dt, \quad (4)$$

where  $\delta(a, b)$  is the Kronecker delta, equal to 1 if  $a = b$  and 0 if  $a \neq b$ , and  $R_t(\epsilon_t, \epsilon_t) = -\sum_{\gamma \neq \epsilon_t} R_t(\epsilon_t, \gamma)$  (Campbell et al., 2024). Therefore,  $p_{t+dt}$  is a Categorical distribution with probabilities  $\delta(\epsilon_t, \cdot) + R_t(\epsilon_t, \cdot)dt$  with notation  $s \sim \text{Cat}(\delta(\epsilon_t, s) + R_t(\epsilon_t, s)dt)$ .

For finite time intervals  $\Delta t$ , a sequence trajectory can be simulated with Euler steps following:

$$\epsilon_{t+\Delta t} \sim \text{Cat}(\delta(\epsilon_t, \epsilon_{t+\Delta t}) + R_t(\epsilon_t, \epsilon_{t+\Delta t})\Delta t). \quad (5)$$

The rate matrix  $R_t$  along with an initial distribution  $p_0$  define CTMC. Furthermore, the probability flow  $p_t$  is the marginal distribution of  $\epsilon_t$  at every time  $t$ , and we say the rate matrix  $R_t$  generates  $p_t$  if  $\partial_t p_t = R_t^T p_t, \forall t \in [0, 1]$ .

In the actual training, Campbell et al. (2024) show that we can train a neural network to approximate the true denoising distribution using the standard cross-entropy:

$$\mathcal{L}_{\text{CE}} = \mathbb{E}_{t \sim \mathcal{U}[0, 1], p_t(\epsilon_t)} [\log p_\theta(\epsilon_1 | \epsilon_t)]. \quad (6)$$

**Rate Matrix for Inference.** The conditional rate matrix  $R_t(\epsilon_t, s | s_1)$  generates the conditional flow  $p_t(\epsilon_t | \epsilon_1)$ . And  $R_t(\epsilon_t, s) = \mathbb{E}_{p_1(\epsilon_1 | \epsilon_t)} [R_t(\epsilon_t, s | \epsilon_1)]$ , for which the expectation is taken over  $p_1(\epsilon_1 | \epsilon_t) = \frac{p_t(\epsilon_t | \epsilon_1) p_1(\epsilon_1)}{p_t(\epsilon_t)}$ . With the conditional rate matrix, the sampling can be performed:

$$\begin{aligned} R_t(\epsilon_t, \cdot) &\leftarrow \mathbb{E}_{p_1(\epsilon_1 | \epsilon_t)} [R_t(\epsilon_t, \cdot | \epsilon_1)], \\ \epsilon_{t+\Delta t} &\sim \text{Cat}(\delta(\epsilon_t, \epsilon_{t+\Delta t}) + R_t(\epsilon_t, \epsilon_{t+\Delta t})\Delta t). \end{aligned} \quad (7)$$

The rate matrix generates the probability flow for discrete variables.

Campbell et al. (2024) define the conditional rate matrix starting with

$$R_t(\epsilon_t, s | \epsilon_t) = \frac{\text{ReLU}(\partial_t p_t(s | \epsilon_1) - \partial_t p_t(\epsilon_t | \epsilon_1))}{N \cdot p_t(\epsilon_t | \epsilon_1)}. \quad (8)$$

In practice, the closed-form of conditional rate matrix with *masking state* [MASK] is defined as:

$$R_t(\epsilon_t, s | \epsilon_1) = \frac{\delta(\epsilon_1, s)}{1 - t} \delta(\epsilon_t, [\text{MASK}]). \quad (9)$$



### B.3 DISCRETE DIFFUSION PROBABILISTIC MODELING

The discrete diffusion models (Austin et al., 2021; Lou et al., 2023; Sun et al., 2022; Campbell et al., 2022; Zheng et al., 2023) can be generally defined by a sequential process of progressive noisy variables  $z_t \in V$  from the categorical variable  $z_0 \in V$ . Denote the one-hot (row) vector of  $z_t$  as  $z_t \in \{0, 1\}^{|V|}$ , in the discrete-time case (Austin et al., 2021), the forward marginal probability of  $z_t$  at time  $t$  has the following form as a composition of Markov kernel defined by  $Q_t$  ( $t = 1, 2, \dots, T$ ):

$$q(z_t|z_0) = \text{Cat}(z_t; z_0 \bar{Q}_t) \triangleq \text{Cat}(z_t; z_0 Q_1 \cdots Q_t), \quad (10)$$

where  $Q_t$  indicates the transition probability matrix for time  $t$  represented by  $[Q_t]_{ij} = q(z_t = j|z_{t-1} = i)$ , and  $\text{Cat}(\cdot; \mathbf{p})$ ,  $\mathbf{p} \in \Delta^{|V|}$  indicates the categorical distribution with probability and  $\Delta^{|V|}$  is the  $|V|$ -simplex. Eq. 10 also induce the form of the marginal distribution for  $\forall t > s$  is  $q(z_t|z_s) = \text{Cat}(z_t; z_s \bar{Q}_{t|s}) \triangleq \text{Cat}(z_t; z_s Q_{s+1} \cdots Q_t)$ . Correspondingly, the posterior  $q(z_s|z_t, z_0)$  can be obtained by the reverse process (Austin et al., 2021):

$$q(z_s|z_t, z_0) = \frac{q(z_t|z_s, z_0)q(z_s|z_0)}{q(z_t|z_0)} = \text{Cat}\left(z_s; \frac{z_t Q_{t|s}^\top \odot z_0 \bar{Q}_s}{z_0 Q_t z_t^\top}\right), \forall s < t. \quad (11)$$

Both Zhao et al. (2024) and Shi et al. (2024) discuss how the discrete-time diffusion process can be generalized to the time domain  $t \in [0, 1]$ , akin to the diffusion over continuous space (Song et al., 2020), by demonstrating the continuous-time limit as  $T \rightarrow \infty$ . Notably, when the stationary distribution is explicitly specified (denoted as  $\mathbf{p} \in \Delta^{|V|}$ ), we can choose a *state-independent* transition kernel in the simple form:  $Q_{t|s} \triangleq [\alpha(s)^{-1}\alpha(t)\mathbf{I} + (1 - \alpha(s)^{-1}\alpha(t))\mathbf{1}\mathbf{p}^\top]$ , thus simplifying the continuous-time forward marginal to:

$$q(z_t|z_s) = \text{Cat}\left(z_t; \frac{\alpha(t)}{\alpha(s)}z_s + (1 - \frac{\alpha(t)}{\alpha(s)})\mathbf{p}\right), \forall 0 \leq s < t < 1, \quad (12)$$

where  $\alpha(t) \in [0, 1]$  is a strictly monotone decreasing function with  $\alpha_0 = 1$  and  $\alpha_1 \rightarrow 0$ . The equation above demonstrates that the discrete diffusion, when defined with an explicit stationary distribution, can be viewed as an interpolation between two categorical distributions controlled by  $\alpha(t)$ . According to Eq. 11, the reverse process of diffusion defined in Eq. 12 takes the following form for the posterior distribution, where  $0 \leq s < t < 1$ :

$$q(z_s|z_t, z_0) = \text{Cat}\left(z_s; \frac{[\mu(t, s)z_t + (1 - \mu(t, s))\lambda_{z_t}(\mathbf{p})\mathbf{1}] \odot [\alpha(s)z_0 + (1 - \alpha(s))\mathbf{p}]}{\alpha(t)\lambda_{z_t}(z_0) + (1 - \alpha(t))\lambda_{z_t}(\mathbf{p})}\right), \quad (13)$$

where  $\mu(t, s) \triangleq \alpha(s)^{-1}\alpha(t) > 0$  and indicator function  $\lambda_{z_t}(\cdot) \triangleq \langle z_t, \cdot \rangle$  for concision.

#### B.3.1 CONDITIONAL MASKED DIFFUSION LANGUAGE MODEL

Masked diffusion (Austin et al., 2021; Lou et al., 2023; Shi et al., 2024; Sahoo et al., 2024; Lu et al., 2024) represents a special case in which the transition includes an ‘‘absorbing state’’, denoted as [MASK]. In this formulation, the stationary distribution in Eq. 10 assigns all probability mass to the unique special token [MASK], such that  $P(z = [\text{MASK}]) = 1$  and  $P(z \neq [\text{MASK}]) = 0$ . For convenience, we define  $\mathbf{p}_M \in \{0, 1\}^{|V|}$  ( $V \triangleq V \cup \{[\text{MASK}]\}$ ) as the one-hot vector representing [MASK]. In masked diffusion, the stochastic forward process maps  $z_0 \rightarrow [\text{MASK}]$  and remains in this state thereafter (i.e., ‘‘absorbing’’). Conversely, the reverse process gradually unmask (denoises) the [MASK] token to produce the data sample  $z_0$ , where  $s < t$ :

$$q(z_s|z_t, z_0) = \text{Cat}(z_s; [\beta(s, t) + (1 - \lambda_M(z_t))(1 - \beta(s, t))]z_t + \lambda_M(z_t)(1 - \beta(s, t))z_0), \quad (14)$$

where  $\beta(s, t) = \frac{1 - \alpha(s)}{1 - \alpha(t)}$  and  $\lambda_M(z_t) = \langle \mathbf{p}_M, z_t \rangle$ . Eq. 14 implies when  $z_t \neq [\text{MASK}]$ , the backward process simply copies the unmasked token by  $z_s \leftarrow z_t$ , i.e.  $q(z_s|z_t, z_0) = \text{Cat}(z_s; z_t)$ ; otherwise the probability mass interpolates between  $\mathbf{p}_M$  and  $z_0$ . The posterior  $q(z_s|z_t, z_0)$  can be approximated by  $p_\theta(z_s|z_t)$  using re-parameterization:  $p_\theta(z_s|z_t) = q(z_s|z_t, \mathbf{u}_\theta(t, z_t))$ , where the neural net  $\mathbf{u}_\theta \in \Delta^{|V|}$  is a neural network that outputs a probability vector that remains in  $\Delta^{|V|}$ .

For inpainting generation, we now consider the conditional case of masked diffusion. Given the amino acid types  $\mathbf{c}$ , our goal is to sample structure tokens through Eq. 14, utilizing a conditional

posterior  $q(\mathbf{z}_s|\mathbf{z}_t, \mathbf{z}_0; \mathbf{c})$ . This posterior can be re-parameterized similarly by incorporating the condition into the backbone model, resulting in  $p_\theta(\mathbf{z}_s|\mathbf{z}_t; \mathbf{c}) = q(\mathbf{z}_s|\mathbf{z}_t, \mathbf{u}_\theta(t, \mathbf{z}_t, \mathbf{c}))$ . To achieve this goal, the reverse process simulated by  $p_\theta(\mathbf{z}_s|\mathbf{z}_t; \mathbf{c})$  must effectively approximate the data distribution  $p(\mathbf{z}|\mathbf{c})$ . A feasible training objective is to optimize the estimation of the conditional ELBO within the continuous-time integral, resulting in the following loss:

$$\mathcal{L}(\theta) = \mathbb{E}_{\mathbf{c}, \mathbf{z}_0} \left\{ \int_{t \in [0,1]} \mathbb{E}_{\mathbf{z}_t \sim q(\mathbf{z}_t|\mathbf{z}_0)} \left[ \frac{1}{1 - \alpha(t)} \frac{\partial \alpha(t)}{\partial t} \lambda_M(\mathbf{z}_t) \log \langle \mathbf{u}_\theta(t, \mathbf{z}_t, \mathbf{c}), \mathbf{z}_0 \rangle \right] dt \right\}, \quad (15)$$

where  $\mathbf{z}_0$  is sampled from the learned encoder  $q_\phi(\mathbf{z}|\mathbf{x})$  with the corresponding amino acid condition  $\mathbf{c}$  from the data distribution  $p(\mathbf{x}, \mathbf{c})$ , and  $\lambda_M(\mathbf{z}_t)$  implies the loss is only applied for the latents  $\forall t$ , s.t.  $\mathbf{z}_t = [\text{MASK}]$ . In practice, we can employ Monte Carlo estimation to compute the integral.

### B.3.2 BIDIRECTIONAL ENCODER AS DENOISING NETWORK

We now discuss the implementation of the conditional denoising network using bidirectional encoder language models, such as BERT (Devlin, 2018). First, consider the sequential generalization of masked diffusion with a sequence of categorical variables. Let  $\mathbf{z}_t$  now be a sequence of discrete structure tokens  $[\mathbf{z}_{t,[1]}, \mathbf{z}_{t,[2]}, \dots, \mathbf{z}_{t,[L]}]$  where  $\mathbf{z}_{t,[i]} \in \bar{V}, \forall i = 1, \dots, L$ . Due to the interpolation scheme of Eq. 12 and Eq. 14, we assume conditional independence and factorize the posterior distribution  $p_\theta(\mathbf{z}_s|\mathbf{z}_t; \mathbf{c})$  across the  $L$  output tokens, such that  $p_\theta(\mathbf{z}_s|\mathbf{z}_t, \mathbf{c}) = \prod_{i=1}^L p_\theta(\mathbf{z}_{s,[i]}|\mathbf{z}_t, \mathbf{c}) = \prod_{i=1}^L q(\mathbf{z}_{s,[i]}|\mathbf{z}_{t,[i]}, \mathbf{u}_{\theta,[i]}(t, \mathbf{z}_t, \mathbf{c}))$  where  $\mathbf{u}_{\theta,[i]}(t, \mathbf{z}_t, \mathbf{c})$  represents the  $i$ -th output channel of neural network. This implement coincides with the BERT-style transformer architecture and allow us to take advantage of existing protein foundation model, for example ESM3 (Hayes et al., 2024). For a sequence of tokens, the masked log-term in the training objective from Eq. 15 is replaced by the summation:  $\sum_{i=1}^L \lambda_M(\mathbf{z}_{t,[i]}) \log \langle \mathbf{u}_{\theta,[i]}(t, \mathbf{z}_t, \mathbf{c}), \mathbf{z}_{0,[i]} \rangle$ , with notations the same as defined above.

**Modifications.** The following are special considerations for the network: (1) *Position-coupled encoding.* Unlike general translation problem, GENZYME maintain strict position-to-position correspondence between amino acid types and the latent tokens<sup>3</sup>. This inductive bias enables us to construct the input embedding for all position  $i$  as follows:  $e_{[i]} = f_\theta[e_z(\mathbf{z}_{t,[i]}) + e_c(\mathbf{c}_{[i]}) + e_t(t)] \in \mathbb{R}^D$ , where  $e_z: |\bar{V}| \mapsto \mathbb{R}^D, e_c: |\mathcal{S}| \mapsto \mathbb{R}^D, e_t: \mathbb{R} \mapsto \mathbb{R}^D$  are the embedding functions and  $f_\theta$  is a linear transformation. (2) *Copying.* The unmasked tokens  $\mathbf{z}_{t,[i]} \neq [\text{MASK}]$  remain the same in spite of the model output. (3) *Zero-out [MASK].* Since  $\mathbf{u}_\theta$  parameterize the approximated clean data  $\mathbf{z}_0$  (fully unmasked), the [MASK] token cannot present in the output and its probability should be zero-out. This is equivalent to adding  $-\infty$  to the logit. In our study, the pre-trained LM head of ESM3 is replaced with a randomly initialized head with augmented vocabulary ( $\bar{V}$ ) during fine-tuning.

## C GENZYME METHOD

GENZYME is an end-to-end, reaction-conditioned, three-stage enzyme design model trained on the EnzymeFill dataset. It includes a catalytic pocket structure generation and sequence design module, a pocket inpainting and enzyme inverse folding module, and a pocket-specific enzyme-substrate binding module. GENZYME generates enzymes conditioned on the SMILES representations of substrates and products, enabling function-driven enzyme design for specific catalytic reactions.

In this section, we discuss the workflow and key components of the GENZYME architecture, including: (1) EnzymeFill and GENZYME training data, (2) the catalytic pocket generation and sequence design module, (3) the catalytic pocket inpainting and enzyme inverse folding module, and (4) the substrate binding and screening module.

### C.1 GENZYME TRAINING DATA

GENZYME is trained on EnzymeFill dataset. EnzymeFill is a curated and validated dataset of enzyme-reaction pairs with valid catalytic pocket structures (Hua et al., 2024b), comprising catalytic reactions collected from the Rhea (Bansal et al., 2022), MetaCyc (Caspi et al., 2020), and Brenda

<sup>3</sup>The underlying co-evolutionary relationships between residues are fully shared across both amino acid types and its spatial patterns.

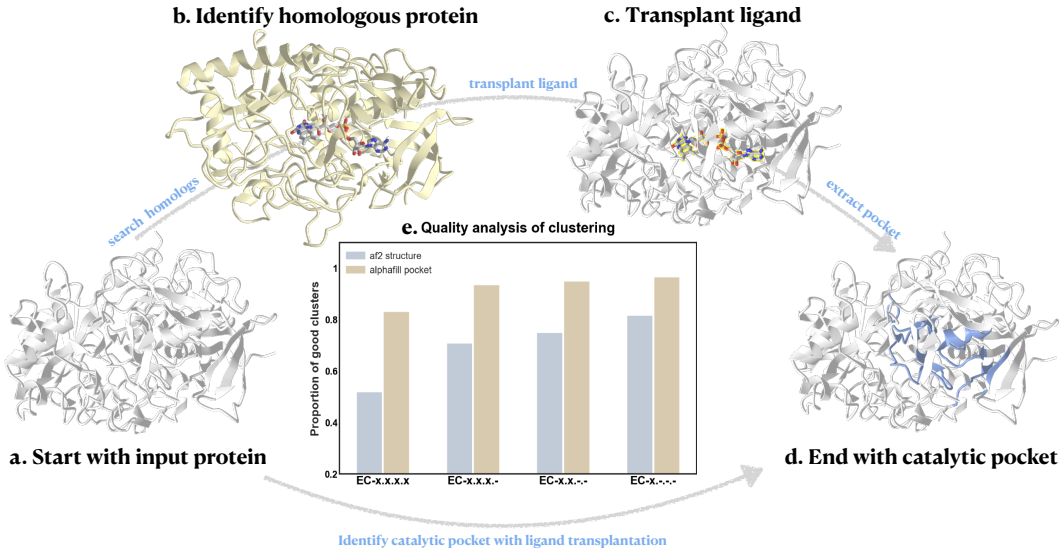


Figure 9: **EnzymeFill dataset construction with ligand transportation.** Starting with (a) an input enzyme structure from AlphaDB (Uniprot P9WMV9), the process (b) identifies a homologous protein in PDB-REDO (PDB 1COY), then (c) transplants ligands from the homologous protein complexes to the target enzyme. (d) A catalytic pocket is identified using a pre-defined radius of 10Å. (e) Quality analysis of clustering between enzyme catalytic pockets and full structures, where strong clusters indicate high functional concentration.

(Schomburg et al., 2002) databases. It contains a total of 328,192 enzyme-reaction pairs, including 145,782 unique enzymes and 17,868 unique reactions.

Catalytic pockets in EnzymeFill are extracted from AlphaDB structures using AlphaFill and ligand transplantation (Hekkelman et al., 2023), as demonstrated in Fig. 9. Fig. 9(e) highlights that enzyme catalytic pockets capture functional information more effectively than full enzyme structures, which supports the approach of focusing on catalytic pocket generation rather than full structure generation.

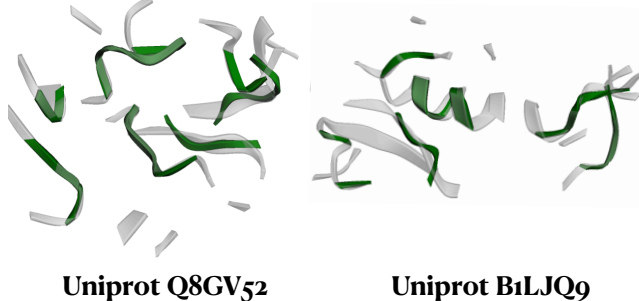


Figure 10: GENZYME use catalytic pockets with 64 residues for training. Grey color shows pockets with 64 residues, green color show pocket with 32 residues.

In GENZYME, enzyme-reaction pairs with fewer than 64 pocket residues are excluded from training. While EnzymeFlow used pockets with 32 residues (their choice is based on LigandMPNN (Dauparas et al., 2023)), the smaller pocket size can result in weaker training signals for learning structural information, such as pairwise distances and angles. Therefore, GENZYME opts for 64-residue pockets to enhance the model’s ability to capture structural details in optimization, as shown in Fig. 10. GENZYME uses a total of 128,940 enzyme-reaction pairs with pocket structures and reaction SMILES for training.

### C.2 POCKET GENERATION AND POCKET SEQUENCE DESIGN MODULE

Conditioned on the input catalytic reaction  $m_r = [m_1, m_2]$ , the pocket generation module of GENZYME generates a catalytic pocket structure  $\mathbf{E}^P$ :

$$\text{POCKETSTRUCT } \mathbf{E}^P \leftarrow \text{PocketGenModule}(\text{SUBSTRATE } m_1, \text{PRODUCT } m_2). \tag{16}$$

The pocket generation module leverages EnzymeFlow (Hua et al., 2024b) to generate catalytic pocket structures. Originally, EnzymeFlow is a conditional flow matching model that co-generates pocket structures, amino acid types, enzyme-reaction co-MSAs, and enzyme commission numbers.

In GENZYME, we first generate catalytic pocket structures  $\mathbf{E}^P$ , while the pocket sequences  $\mathbf{A}^P = \{a_1, \dots, a_{N_P}\}$  is co-generated using a pocket inverse folding head. However, during training, we still encode and predict masked amino acid types and enzyme-reaction co-MSAs for the purpose of masked autoencoder loss, while enzyme commission numbers are omitted. In addition to flow-matching losses on SE(3) frames and pairwise distance losses from Hua et al. (2024b), GENZYME incorporates more restricted geometric regularization techniques, including FAPE loss, LDDT loss, TM loss, and violation loss as proposed in Jumper et al. (2021); Ahdritz et al. (2024), to enhance the structural accuracy of generated pockets:

$$\mathcal{L}_{\text{FAPE}} = \frac{1}{N_P} \sum_{i=1}^{N_P} \left\| E_i^P \mathbf{p}_i - \hat{E}_i^P \hat{\mathbf{p}}_i \right\|^2, \mathcal{L}_{\text{LDDT}} = \frac{1}{N_P} \sum_{i=1}^{N_P} \left( \frac{1}{|\mathbf{N}(i)|} \sum_{j \in \mathbf{N}(i)} \frac{1}{1 + \left( \frac{d_{ij} - \hat{d}_{ij}}{d_0} \right)^2} \right), \quad (17)$$

$$\mathcal{L}_{\text{TM}} = \frac{1}{N_P} \max \left( \sum_{i=1}^{N_P} \frac{1}{1 + \left( \frac{d_i}{d_0} \right)^2} \right).$$

Here, in  $\mathcal{L}_{\text{FAPE}}$ ,  $\hat{E}^P$  denotes the predicted pocket residue frame, and  $\mathbf{p}_i$  and  $\hat{\mathbf{p}}_i$  represent the true and predicted Euclidean atom positions in the residue frame, respectively. In  $\mathcal{L}_{\text{LDDT}}$ ,  $\mathbf{N}(i)$  refers to the set of neighboring residues of the  $i$ -th residue, and  $d_{ij}$  and  $\hat{d}_{ij}$  are the true and predicted distances between residues  $i$  and  $j$ , with  $d_0 = 10\text{\AA}$  as a threshold. In  $\mathcal{L}_{\text{TM}}$ ,  $d_i$  is the distance between the  $i$ -th residue pair in the true and predicted structures, and  $d_0$  is scaled as  $d_0 = 1.24\sqrt{N_P - 15} - 1.8$ , following Jumper et al. (2021). Additionally, the violation loss penalizes deviations in bond lengths, angles, and steric clashes within the predicted pocket frames.

To further improve generalizability, we relax the substrate conformation assumption from EnzymeFlow. While EnzymeFlow conditions pocket generation on pre-computed substrate conformations, we use a 2D graph representation of the substrate molecule, allowing GENZYME to work even when the optimal substrate conformation for a catalytic reaction is unknown. This enhances the flexibility and applicability of the model across various reactions.

GENZYME also generates the pocket sequence  $\mathbf{A}^P$  for the pocket structure  $\mathbf{E}^P$ :

$$\begin{aligned} \text{POCKETSEQ } \mathbf{A}^P &\leftarrow \text{PocketInvFoldModule}(\text{POCKETSTRUCT } \mathbf{E}^P), \\ \text{POCKET } \mathbf{E}^P &\leftarrow \text{Integrate}(\text{POCKETSTRUCT } \mathbf{E}^P, \text{POCKETSEQ } \mathbf{A}^P). \end{aligned} \quad (18)$$

While structure-sequence co-design has become more popular in recent protein design models, simply adding a naive amino acid prediction head to the model can be insufficient for capturing the important structural and neighborhood information necessary for accurate sequence design. An inverse folding head, on the other hand, captures more structurally meaningful information by leveraging message passing between both neighboring and long-range residues.

For sequence co-design, we enhance the model by replacing the naive amino acid prediction head with an inverse folding head powered by PiFold (Gao et al., 2022). PiFold excels in inference speed compared to other methods, such as ProteinMPNN (Dauparas et al., 2022) and ESM-IF (Lin et al., 2022). We pre-train the pocket inverse folding module on the CATH-4.2 dataset (Sillitoe et al., 2021) and then fine-tune it on EnzymeFill pocket data. In GENZYME, the fine-tuned inverse folding head is integrated for end-to-end catalytic pocket design. This involves using cross-entropy loss between the predicted sequences of the generated pockets and the true sequences of true catalytic pockets, ensuring accurate sequence generation and refinement.

### C.3 CATALYTIC POCKET INPAINTING AND ENZYME INVERSE FOLDING MODULE

Following the catalytic pocket generation, where the active site predominantly determines the enzyme function, GENZYME inpaints the pocket structure  $\mathbf{E}^P$  into a full enzyme structure  $\mathbf{E}$ :

$$\text{ENZYMESTRUCT } \mathbf{E} \leftarrow \text{PocketInpaintModule}(\text{POCKET } \mathbf{E}). \quad (19)$$

While the catalytic pocket is important to enzyme function—serving as the active site for substrate binding and catalysis—inpainting the catalytic pocket into a full enzyme structure is essential

for overall enzyme stability, proper folding, and determining other properties (Robinson, 2015). GENZYME fine-tunes ESM3 (Hayes et al., 2024) on EnzymeFill for catalytic pocket inpainting, it can inpaint catalytic pockets and predict enzyme sequences through Gibbs or discrete diffusion processes (Lu et al., 2024). Although other models like RFDiffusion (Wang et al., 2022) and Genie2 (Lin et al., 2024) could also be employed<sup>4</sup>. ESM3 is chosen for its faster inference speed, and we are exploring an additional approach of training our own generative inpainting model.

**EnzymeESM with Pocket-specified Hierarchical Fine-tuning.** To enhance performance on enzyme structures, it is necessary to fine-tune existing large protein models on catalytic pockets for inpainting, as current models may randomly mask residues during training, including those that are less functionally relevant and not involved in catalysis. Therefore, we introduce EnzymeESM, which fine-tunes ESM3 on the EnzymeFill dataset with a hierarchical fine-tuning approach. Initially, we fine-tune the model by randomly masking residues across the entire enzyme structure, followed by targeted fine-tuning where only the residues that are not belong to catalytic regions are masked for training. In GENZYME, this fine-tuned EnzymeESM is integrated for end-to-end catalytic pocket inpainting. During training, we not only optimize the catalytic pocket to match the true pocket but also teach-forcing the inpainted full enzyme to align with the true enzyme structure. This dual optimization enables GENZYME to generate full enzymes with improved stability, proper folding, and enhanced pocket specificity.

Additionally, EnzymeESM is used to co-design pocket sequences over the full enzyme structure and is further optimized in GENZYME for end-to-end enzyme generation, as:

$$\begin{aligned} \text{ENZYMESSEQ } \mathbf{A} &\leftarrow \text{EnzymeInvFoldModule}(\text{ENZYMESTUCT } \mathbf{E}), \\ \text{ENZYMES } \mathbf{E} &\leftarrow \text{Integrate}(\text{ENZYMESTUCT } \mathbf{E}, \text{ENZYMESSEQ } \mathbf{A}). \end{aligned} \quad (20)$$

GENZYME designs enzymes by generating catalytic pockets and inpainting them to full structures through dual optimization. This approach ensures that GENZYME accurately generates both the enzyme structure and sequence, optimizing substrate specificity and enabling the catalysis for potentially unseen reactions.

#### C.4 POCKET-SPECIFIC ENZYME-SUBSTRATE BINDING MODULE

GENZYME predicts and optimizes the substrate molecule conformation  $m_1$  given the catalytic pocket  $\mathbf{E}^P$ , and followed by generating the enzyme-substrate complex  $\mathbf{C}$ , as:

$$\text{COMPLEX } \mathbf{C} \leftarrow \text{BindingModule}(\text{ENZYMES } \mathbf{E}, \text{SUBSTRATE } m_1). \quad (21)$$

The enzyme-substrate binding module is the only component in GENZYME that is not trained end-to-end. However, during sampling and inference, the binding module operates end-to-end. It cannot be trained this way due to current data limitations: the substrate conformations computed by AlphaFill are not guaranteed optimal, thus directly using these conformations can result in binding poses with serious atomic clashes. Addressing this data limitation—specifically, identifying the optimal enzyme-substrate binding poses—is a key challenge that GENZYME aims to solve. Once the binding poses are validated as being at their optimal geometries<sup>5</sup>, we can establish a feedback loop, using data generated by GENZYME to train an enzyme-substrate co-generation model like AlphaFold3 (Abramson et al., 2024) using techniques like diffusion or flow matching.

GENZYME incorporates Uni-Mol Docking v2 (Alcaide et al., 2024) in its pocket-specific enzyme-substrate binding module. Uni-Mol Docking v2 is selected for its strong performance in predicting binding poses with low distance errors, consistently outperforming AlphaFold-latest on benchmarks like PoseBusters (Buttenschoen et al., 2024). Within the binding module, multiple substrate conformations are computed and further optimized within the catalytic pocket. GENZYME then outputs the predicted enzyme-substrate complex with the lowest affinity scores.

<sup>4</sup>Although developing a pocket inpainting model from scratch would be novel from an algorithmic standpoint, it is not necessary, as these protein models are well-trained and optimized on millions of protein representations. Fine-tuning them for downstream applications, *e.g.*, enzymes, is sufficient for domain-specific usage.

<sup>5</sup>Although GENZYME can predict enzyme-substrate binding poses with computationally optimal affinities, experimental validation, such as wet-lab assays, is required to ensure the predicted binding poses are within an acceptable RMSD range (*e.g.*, 2Å), similar to how DeepMind demonstrated the accuracy of AlphaFold-predicted structures through RMSD and distance evaluation.

## D VISUALIZATION

## D.1 BASELINES

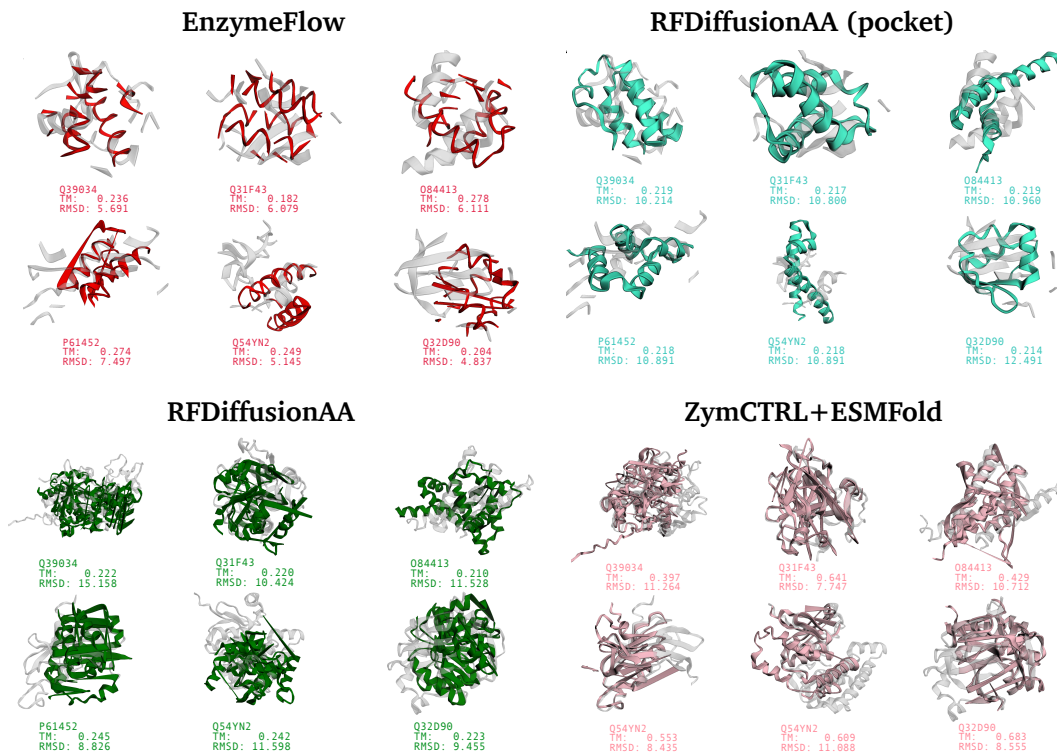


Figure 11: Baseline visualizations including EnzymeFlow, RFDiffusionAA (pocket), RFDiffusionAA, and ZymCTRL+ESMFold. These visual examples are selected by best TM-score. The ground-truth samples are shown in gray, and generated samples are colored.

## D.2 POCKET DESIGN WITH GENZYME

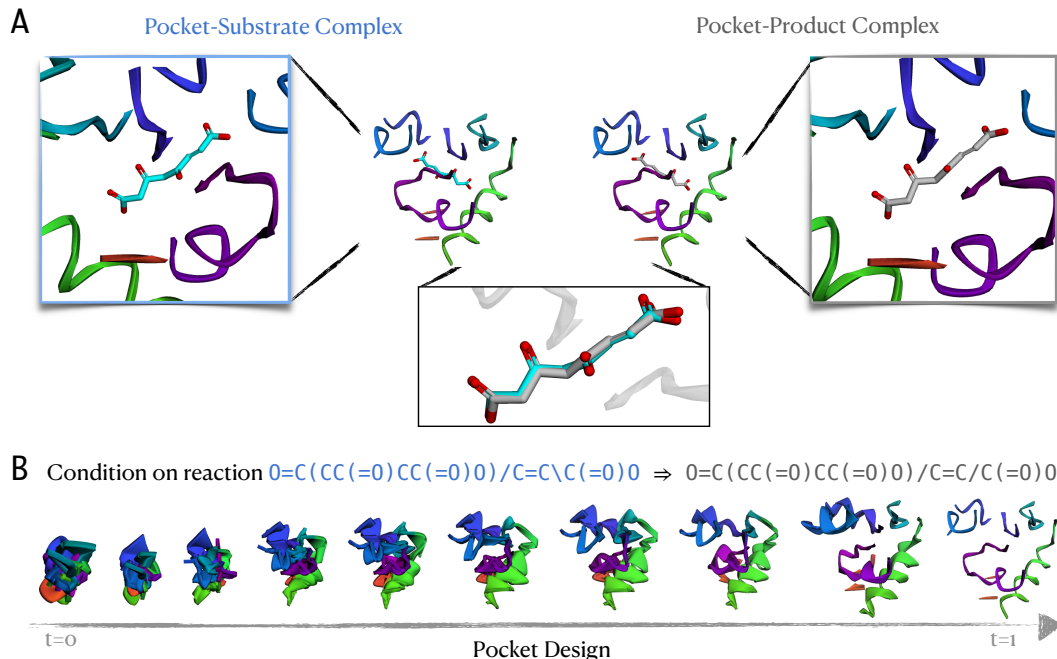


Figure 12: Catalytic Pocket Design with GENZYME.

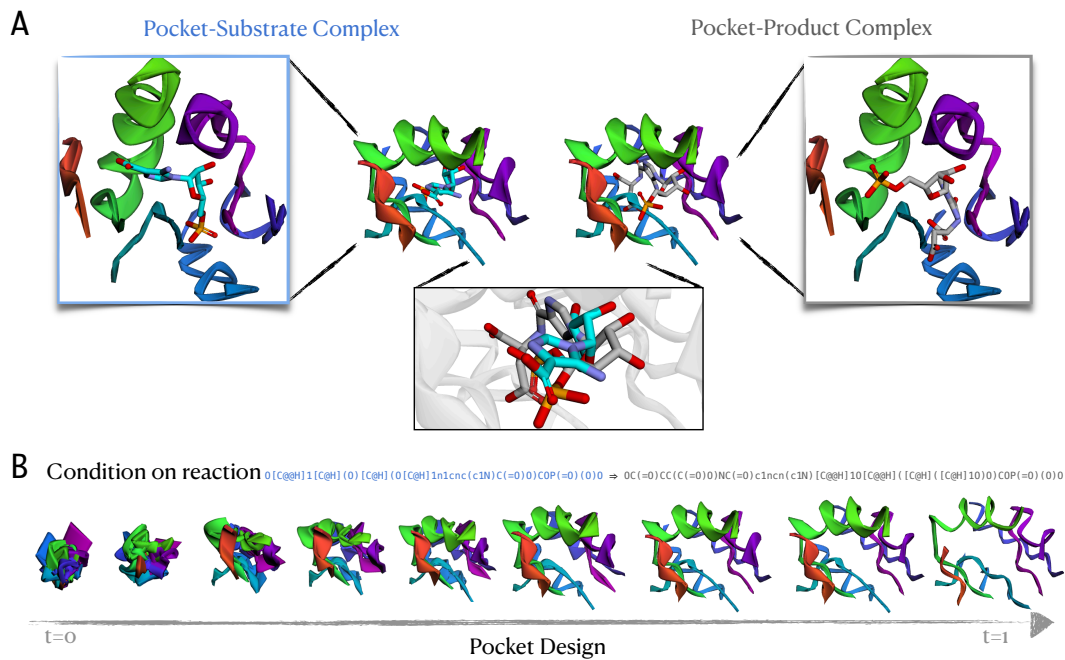


Figure 13: Catalytic Pocket Design with GENZYME.

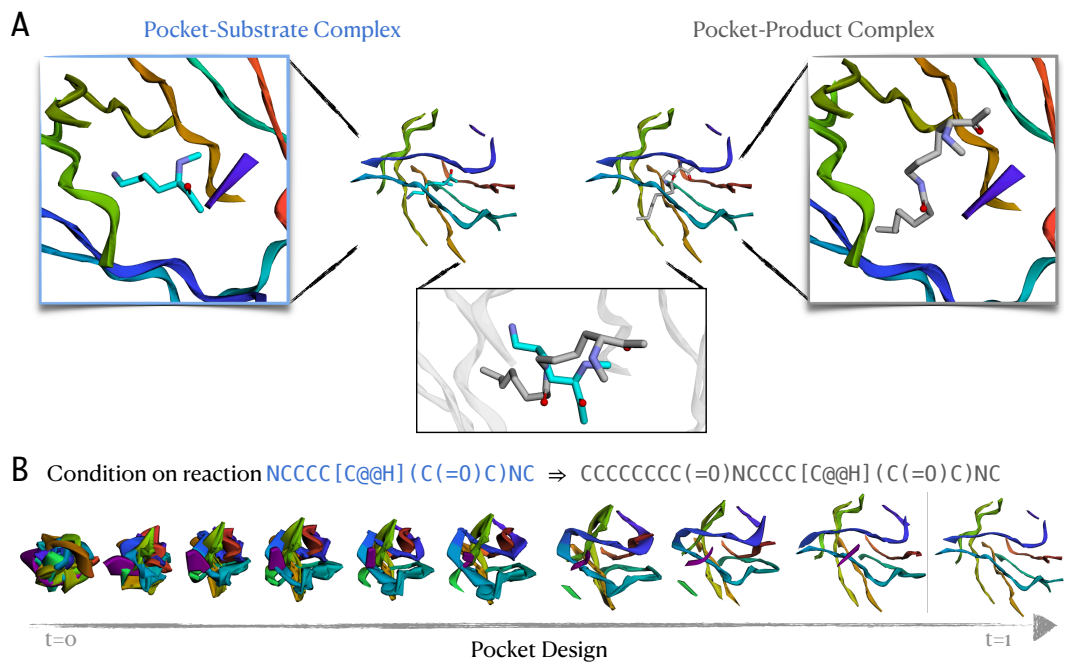


Figure 14: Catalytic Pocket Design with GENZYME.